

**COMPARISON OF OPEN SOURCE TUMOR GROWTH
SIMULATION SOFTWARE AND MULTISCALE TUMOR
MODELLING**

by

Ahmet Fırat akmak

B.S., in Bioengineering, Yıldız Technical University, 2014

Submitted to the Institute of Biomedical Engineering
in partial fulfillment of the requirements
for the degree of
Master of Science
in
Biomedical Engineering

Boğaziçi University

2020

**COMPARISON OF OPEN SOURCE TUMOR GROWTH
SIMULATION SOFTWARE AND MULTISCALE TUMOR
MODELLING**

APPROVED BY:

Assoc. Prof. Dr. Albert Güveniş
(Thesis Advisor)

Assist. Prof. Dr. Daniela Schulz

Assist. Prof. Dr. Mehmet Kocatürk

DATE OF APPROVAL: 21 May 2020

ACKNOWLEDGMENTS

I would first like to thank my advisor Assoc. Professor Dr. Albert Güveniř of the Institute of Biomedical Engineering at Bogazici University for his continuous support and guidance during my thesis.

I would like to thank my wife Eda for always making me feel her support whenever I may need it.

Thank you to my cousin Assoc. Professor Dr. Ayca Cakmak Pehlivanli for devoting her time and information to me, both are very valuable for me.

Also, I want to thank my friend Taha Hasekioglu for always keeping me motivated to complete this thesis.

ACADEMIC ETHICS AND INTEGRITY STATEMENT

I, Ahmet Fırat akmak, hereby certify that I am aware of the Academic Ethics and Integrity Policy issued by the Council of Higher Education (YÖK) and I fully acknowledge all the consequences due to its violation by plagiarism or any other way

Name :

Signature:

Date:

ABSTRACT

COMPARISON OF OPEN SOURCE TUMOR GROWTH SIMULATION SOFTWARE AND MULTISCALE TUMOR MODELLING

Cancer is a complex disease that is comprised of many different cellular and tissue level organizations. Tumor growth simulation is vital in predicting the way tumors grow. Tumor modelling is used to shed light on cancer biology and is considered a promising method for developing more effective cancer therapies. In this study, the biological inputs and their respective outputs using the simulation approaches were systematically reviewed. A comparison table was produced that shows in detail the biological inputs for each simulation code. This is in contrast to the current agent-based model reviews that mostly focus on computer efficiency. Physicell was selected among the reviewed open-source software due to its integrated basic cell functions and microenvironment simulation capabilities. Tumor growth has been simulated in the Physicell v1.6.1 tumor simulation software. The A549 cell specific parameters have been used during the simulation and the effects of the initial oxygen concentration in the microenvironment were examined on outcome images. Growth rate of tumor cells increases with the increasing oxygen concentration in the microenvironment. Formation rate of necrotic core in the tumor structure reduces with the increasing oxygen concentration due to small number of hypoxic cells in the tumor structure. Based on our findings in the simulation, physicians can predict the hypoxic regions in tumor structure to plan a chemotherapy treatment dependent localized peripheral tissue considering the correlation between oxygen concentration and tumor growth rate.

Keywords: Cancer, Tumor Growth, Agent-Based Model Simulations.

ÖZET

AÇIK KAYNAK TUMOR BUYUME SİMULASYON PROGRAMLARININ KARŞILAŞTIRILMASI VE ÇOK OLÇEKLİ TUMOR MODELLENMESİ

Kanser, birçok farklı hücresel ve doku seviyesi organizasyonundan oluşan karmaşık bir hastalıktır. Bu değişkenler kanser ve tümör büyümesini tahmin etmeyi zorlaştırır. Tümör büyüme simülasyonu, tümörlerin büyüme şeklini tahmin etmede hayati öneme sahiptir. Tümör modelleme, kanser biyolojisine ışık tutmak için kullanılır ve daha etkili kanser tedavileri geliştirmek için umut verici bir yöntem olarak kabul edilir. Literatürdeki çalışmalardan farklı olarak, belirtilen simülasyon yöntemlerini kullanarak biyolojik ve metabolik girdiler ve bunların ilgili çıktıları sistematik olarak gözden geçirilmiştir. Her bir simülasyon kodu için biyolojik girdileri ayrıntılı olarak gösteren bir karşılaştırma tablosu oluşturulmuştur. Sistematik olarak gözden geçirilmeden sonra ek olarak, bütünleşik hücre fonksiyonları ve mikro çevre özellikleri nedeniyle Physicell v1.6.1 programında, adenocarcinoma A549 hücrelerine ait hücre parametreleri kullanılarak tümör büyümesi gözlemlenmiştir. Ayrıca, ortamdaki başlangıç oksijen konsantrasyonunun, tümör büyümesine etkisi incelenmiştir. Tümör hücrelerinin oluşum hızı, başlangıçtaki oksijen konsantrasyonu artmasıyla, artmıştır. Bununla birlikte, nekrotik ve ona ait kalsiyum bazlı yapının oluşumu, hipoksik hücrelerde azalmaya bağlı olarak, artan oksijen miktarıyla azalmıştır. Simülasyon bulgularına istinaden, araştırmacılar tümör yapısındaki hipoksik bölgeleri öngörerek, hastaya özel uyarlanmış kemoterapi planlarını belirleyebilirler.

Anahtar Sözcükler: Kanser, Tümör Büyümesi, Ajan Tabanlı Modelleme.

TABLE OF CONTENTS

ACKNOWLEDGMENTS	iii
ACADEMIC ETHICS AND INTEGRITY STATEMENT	iv
ABSTRACT	v
ÖZET	vi
LIST OF FIGURES	ix
LIST OF TABLES	x
LIST OF SYMBOLS	xi
LIST OF ABBREVIATIONS	xii
1. INTRODUCTION and MOTIVATION	1
2. BACKGROUND AND THEORY	3
2.1 Cancer Biology and Cell Proliferation	3
2.2 Agent Based Models (ABM) for Tumor Growth Simulation	8
3. LITERATURE SEARCH	11
3.1 Open Source Softwares for Tumor Growth Simulations in the Literature	11
4. METHODS	20
4.1 Comparison Method and Search Strategies for Open Source Tumor mod- eling Softwares	20
4.2 Integration of Models for Diagnosis and Prediction of Cancer Treatment	21
4.3 Tumor Growth Simulation in PhysiCell v1.6.1	22
4.4 Physicell v1.6.1 Working Principle and Software Features	23
4.5 Overall Simulation Working Principle	24
4.6 Biochemical Microenvironment	25
4.7 Cell Volume	26
4.8 Cell Cycle General Rule	27
4.8.1 Cell Division	27
4.8.2 Flow Cytometry Separated Cell Cycle Model	28
4.8.3 Oxygen-dependent phenotype	29
4.8.3.1 Overall model for proliferation	30
4.8.3.2 Overall model for necrosis	30

4.9	Cell Coloring in Simulation Output	31
4.10	Evaluation Method	32
5.	RESULTS	33
5.1	Comparison of Open Source Software based on Literature Research	33
5.2	Tumor Growth Simulation	36
5.3	Effect of Initial Oxygen Concentration in the Tumor Microenvironment	41
5.4	Effect of Initial Oxygen Concentration on the Tumor Growth Rate	43
6.	DISCUSSION	45
6.1	Main Findings	45
6.2	Clinical Applications and Benefits	46
6.3	Limitations	47
7.	CONCLUSIONS	48
	APPENDIX A. General Code Structure of Tumor Growth Simulation	50
	REFERENCES	51

LIST OF FIGURES

Figure 2.1	Cell Cycle Stages.	3
Figure 2.2	Necrotic Core of Tumor Structure.	6
Figure 2.3	Cell and fluid flux during the tumor growth progression.	7
Figure 2.4	Illustration of lattice based(left) and off lattice based(right) simulation models.	10
Figure 3.1	Oxygen Concentration in the Growing Tumor Spheroid.	12
Figure 3.2	Wilensky's Tumor Model in Netlogo.	13
Figure 3.3	Tumor growth simulation in Repast. The green, blue and red dots represents tumor cells and yellow shades shows nutrient concentration.	13
Figure 3.4	Avascular cell proliferation in two dimensional (upper part) and three dimensional.	15
Figure 3.5	Vascular 3D model of stem cells. Green section represents tumor cells. Red parts are blood vessels and yellow parts are new blood vessels.	15
Figure 3.6	Tumor simulation in FLAME. Blue colors represent tumor cells and red dots represent blood vessels.	18
Figure 4.1	Illustration of Flow Cytometry Separated Cell Cycle Model.	28
Figure 5.1	3-D Tumor Growth Structure. Yellow cells represent proliferated cells, red cells are apoptotic cells and brown cell are necrotic cells.	41
Figure 5.2	Tumor Growth Rate at 38 mmHg and 50 mmHg Initial Oxygen Concentration.	43

LIST OF TABLES

Table 2.1	Estimated Oxygen Levels in Tumor and Normal Cells.	5
Table 4.1	Reference Parameters for Cell Volume.	27
Table 4.2	Cell Cycle Reference Durations.	29
Table 4.3	Oxygen Dependent Phenotype Reference Values.	31
Table 4.4	Coloring of SVG outputs for each cell type in the Tumor Structure.	31
Table 5.1	Comparison of Open Source Software Considering Their Inputs and Outputs.	34
Table 5.2	Tumor Growth That Includes A549 Cells Over Time.	36
Table 5.3	Oxygen Distribution in the Tumor Microenvironment Over Time.	42
Table 5.4	Tumor Structure that comprises 150.000 A549 Cells at 38 mmHg and 50 mmHg Initial Oxygen Concentration.	44

LIST OF SYMBOLS

D	Diffusion Coefficient
r_{ij}	Cell Cycle Transition Rates
V	Cell Volume
X_n	Cell Cycle Phase
λ	Decay Rate
ρ	Substrate Concentration
σ	Oxygen Concentration at The Center
Ω	Cartesian Mesh

LIST OF ABBREVIATIONS

A549	Adenocarcinomic Human Alveolar Basal Epithelial Cells
ABM	Agent Based Model
CA	Cellular Automata
CBM	Center Based Model
CPM	Cellular Potts Model
ECM	Extracellular Matrix
LGCA	Lattice Gas Cellular Automata
ODE	Ordinary Differential Equation
PDE	Partial Differential Equation
TSG	Tumor Suppressor Gene

1. INTRODUCTION and MOTIVATION

This aim of this thesis is to compare the open source simulation software to guide researchers by to select an appropriate simulation environment for their studies and create a simulation environment to develop tumor growth to understand the variables that affect tumor progression. Researchers use such simulation environments in the prediction and diagnosis of cancer disease. Recently tumor modelling and cancer diagnosis is an emerging field which aims to prevent the disease in early phase by applying targeted cancer drugs as personalized and predictive medicine. This approach has proven to be a difficult task due to complexity of cancer and the many factors that induce the tumor progression. Tumor simulations can be of use in developing tumor models to understand the factors in tumor progression and the effect of each factor during the progression of cancer

The main goals of this thesis are;

- The systematic review of open source software for the simulation of tumor growth including their inputs, model parameters, pros cons and the outputs. Based on the review, inputs that are used in the literature are sorted to give a concrete pathway for the researchers to select the right open software related with their study field. Researcher can select the right software considering the input (intratumor heterogeneity, cell proliferation, tumor microenvironment etc.) that is encoded in the software. Additionally, outputs of the software are investigated to guide researchers based on their study need. Researcher may select the software in terms of output features (vascular or avascular tumor modelling, three-dimensional or two-dimensional, maximum tumor size, detailed tumor morphology or only tumor progression etc.). Unlike the reviews in the literature, our study aims to compare the biological inputs and outputs that are used in the open softwares in our systematic review as novelty.
- To perform a tumor growth simulation using A549 adenocarcinoma cell specific

parameters using an open software based on the systematic review. We aim to reach in the simulation approximately 1000 μm tumor radius to analyze the proliferative cells, necrotic core and hypoxic regions in the simulation. Moreover, the effects of inputs in the microenvironment are investigated on the tumor growth to enlighten the tumor growth rate based on the different inputs in the microenvironment and how a single change in the input would affect the output. Additionally, tumor growth rate, hypoxic regions and necrotic core will be considered in the simulation environment. Hence, physicians may use the simulations based on our results to investigate the potential tumor growth rate and the effects of hypoxic and necrotic regions in the tumor structure. Since, there is a certain relationship between tumor growth rate, hypoxic regions and the treatment of cancer disease with chemotherapy agents and surgery [1],[2],[3]. In the literature, there is no simulation in three-dimensional and approximately 1000 μm tumor radius using a549 cell specific parameters.

2. BACKGROUND AND THEORY

2.1 Cancer Biology and Cell Proliferation

Cancer biology that is comprised of many different dynamic and complex biological interactions at many scales that are starting from cellular and molecular level and up to tissue and organ levels. In these scales, tumor cells are affected by different biological systems such as mutation, cell signaling, cell proliferation, immune response and substrate concentration and diffusion.

Control of cell division is dependent on certain checkpoints and phases called as cell cycle as shown in Figure 2.1 [4]. First phase is the G1 that is the preparation phase that cell initiates to prepare necessary organelles and proteins for the cell division. Also, the cell organizes the processes related DNA replication. G1 phase is followed by S phase with copy of DNA structure. And then, Nucleus regulates itself for the division of the cell in the G2 phase. Final phase is the M phase for the cell division. Mitosis is occurred in the M phase and the replicated DNA into two different structure with their correspondence DNA. Moreover, cell organelles and cytoplasm are separated into two different cells that represent completely similar features [4].

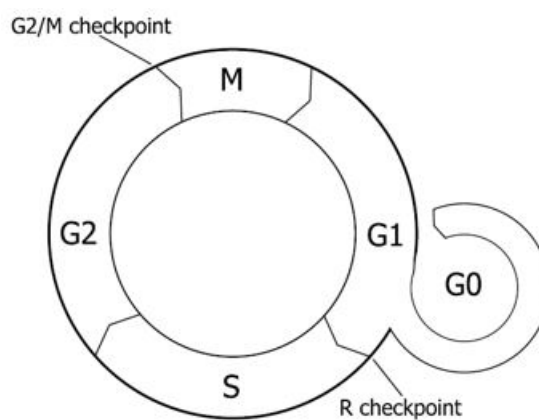


Figure 2.1 Cell Cycle Stages.

Cell cycle and cell growth is regulated with the certain inhibitory signals and these signals are the main parameter that maintain cell growth decision with the secretion level of them. Cell proliferation is managed by two different signals which are promoting and inhibiting signals. Promoting signals trigger the cell proliferation and these signals are led by Oncogenes. Inhibiting signals cause the termination and suspension of cell cycle. And these signals are controlled by Tumor suppressor genes (TSGs). TSGs also carry out proper DNA repair and apoptosis is activated by TSGs if DNA repair is not properly managed. Tumor growth and cancer initiations are occurred with the mutation and anomaly of the both oncogenes and TSGs. Anomaly in these genes cause the unprogrammed signals in the cell division and the disruption of the checkpoint that is responsible with the apoptosis of the cell [4]. Recent searches in the literature shows that there are multiple reasons which cause the mutation and anomaly in the genes that regulates the inhibiting and promoting signals. One of the main reasons is the viral infections that transmit its own DNA/RNA into healthy cell and transform the genes inevitably in the health cells. Also, microenvironmental conditions can affect the genes that are responsible for the cell proliferation. Such as hypoxia can directly affect the cell signaling with overexpression of HIF1- α .

In some cases, internal protein levels can affect gene expression without any external receptor signaling. For example, when hypoxia occurs in a cell, HIF1- α , a hypoxia-inducible factor created by all cells, cannot be degraded due to a lack of oxygen. This low-oxygen environment causes an accumulation of HIF1- α , which activates downstream target genes [5]. Particularly, HIF1- α accumulation upregulates motility and the secretion of angiogenic promoting factors. The low oxygen environment also causes anaerobic glycolysis in the cell. In this case, glucose reacts with glucose instead of oxygen, reducing the cell's metabolic efficiency. Inefficient glucose metabolism causes a reduction in cell-cell and cell-ECM adhesion, making the cells less sensitive to apoptotic signals. So, the hypoxic cells end up promoting angiogenesis and reducing apoptosis without any need for additional receptor signaling. General oxygen concentrations in the human body are given below Table 2.1 [1],[2].

Table 2.1
Estimated Oxygen Levels in Tumor and Normal Cells.

mmHg	% Oxygen	Description
760	100.0	Atmospheric pressure
160	21.0	Level of oxygen in the atmospheric pressure
100	13.5	Oxygen pO_2 in Lung alveoli
70	9.5	Oxygen concentration in the arteries
50	6.5	Oxygen concentration in the venous
38	5.0	Physiological oxygen level in peripheral tissues
15	2.0	The lower level at normal hypoxic responses
8	1.0	Hypoxia level at the peripheral tissues

Ischemic tissue can cause large tumors which will cause the ATP decrease and ceases to death of the cells on that tissue in the same way of continuous lack of oxygen (hypoxia) together with low blood sugar levels. This spontaneous cell death is designated as necrosis. Meanwhile a cell alters to necrotic, the ions locate on the surface stall their function and this results in diffusion of water towards the cell. This water diffusion causes cell to swell and consequential cell burst. This incident is distinguished from apoptosis as the loss of the volume is uniform and the material between cells are encompassed in apoptotic bodies. For the necrotic cells, the solid-cell division is not usually engulfed (via phagocytosis) with the encompassing cells, because commonly they are necrotic on their own. In several cancer types (for instance ovarian, liver, breast cancer and lymphoma), and other pathological conditions (for instance abscesses and tuberculosis), the tissue that is necrotic might undergo calcification. In this incident, molecules of calcium phosphate along with calcium oxalate that attach together for forming crystals of calcite. This union develops into microcalcifications which replaces the solid-cell components [4]. Since a tumor transforms into in-situ cancer, the initial phase of the growth can initiate after the tumor can create a foothold in its host tissue [6].

The basement membrane can usually restrain the epithelial cells. The tumor does not possess a vascular system during this initial phase of cancer. That's why it

needs the host vasculature system in terms of the oxygen, nutrients, and growth factors which can be mentioned as "substrates" of the closest stroma. Substrates can spread from the surrounding vascularized tissue, get into the tumor, and be consumed by proliferating tumor cells. The reason for comprising of the substrate gradients within the tumor is the kinesis of them from the vasculature system of the neighboring tissues) to the interior sinks which are the active tumor cells in terms of their metabolism. Considering the metabolic activities of the cells, one of the significant aspects is the oxygen which can spread into the tissues prior to fall in the inadequate level. This diffused oxygen range is observed usually as 100-200 μm . Interior tumor cells can encounter hypoxia and react to the severe microenvironment in several ways. If the oxygen and glucose of the tumor cells fall down to the insufficient levels, the tumor cells can be necrosed. These dynamics can be observed as an external tumor viable edge of the proliferating cells, an inside line of hypoxic cells, and a main necrotic core shown in Figure 2.2 [4].

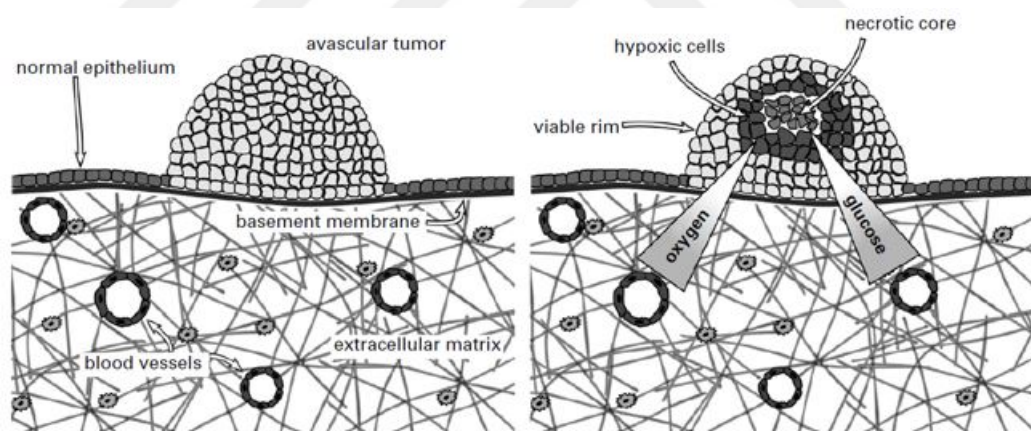


Figure 2.2 Necrotic Core of Tumor Structure.

The mechanical forces caused by the way tumor cells grow and divide, affect how the tumor will grow. Cell proliferation in the tumor causes an outward cell flux. Concurrently, as growing tumor cells on the rim of the tumor absorb fluid from the interstitial space between the tumor and tissue to grow and divide, there is a fluid flux into the tumor. These two phenomena result in cell lysis in the core of the tumor, forming what is called a necrotic core. As the necrotic core forms, the cell volume of the tumor decreases, and the fluid release from cell lysis moves from the necrotic

core to the rim of the tumor. The reduction in mechanical pressure in the necrotic core cause viable cells in the rim to flux to the interior of the tumor, increasing the necrotic core's volume. The increase in the necrotic core's volume results in what is called the cell volume sink effect. As the tumor reaches a certain size, the cell flow from new cells is balanced with the fluid flux from necrosis, resulting in zero outward cell growth as illustrated in Figure 2.3 [4]. The resulting tumor is called a steady-state tumor spheroid.

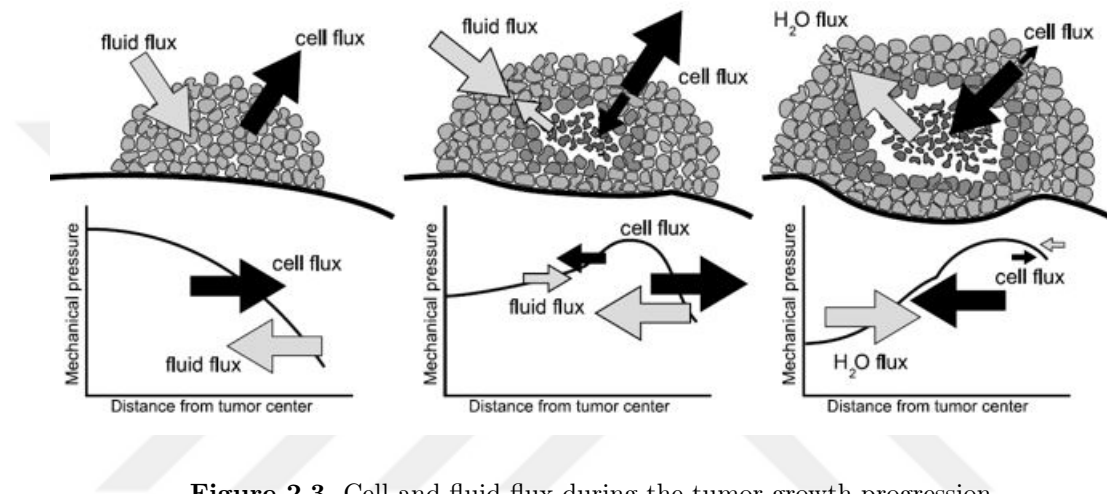


Figure 2.3 Cell and fluid flux during the tumor growth progression.

The tumor-tissue system is a complex system where the tumor and the microenvironment around it are in continual and changing interaction [7]. Biochemical and biophysical processes between the tissue and microenvironment shape each others' behavior. Thus, tumor growth must be studied in a 3-D multicellular system under these conditions. It should be understood that the tumor can reshape the microenvironment directly, through processes such as matrix remodeling, and indirectly, through processes such as secreted signals [8]. Concurrently, the microenvironment shapes the way tumor cells behave. These conditions make experimentation of tumor growth through experiments difficult, even with innovations in biomimetics, tissue engineering, and animal models making computational models an optimum platform to test ideas. Such a platform should allow researchers to simulate the life cycle and motions of tumor cells, the biochemical environment, biomechanics of cells and the ECM, the changing vasculature, and the interstitial and microvascular flow.

2.2 Agent Based Models (ABM) for Tumor Growth Simulation

Simulating cancer cells also known as cell-based or agent-based models. Agent based models are mainly classified as lattice based and off lattice based [9]. They are focus on the individual cell behavior and its surrounding tissue. Agent based models possess many benefits. In this simulation software, heterogeneity in cancer can be modeled where each cell agent be used to follow a fully independent state with individual parameters. The cell behaviors which are individual cell mechanisms and interactions between cell and extracellular matrix can be executed in the simulation environment that enable us to quickly translate biological accepted processes into mathematical rules [10].

Models based on lattices may use standard structured meshes [2D/3D]. Structured meshes are easier to execute, display, and unify with the equation solvers, but their design can result in grid faults [11]. These problems can be avoided by unstructured meshes, but with greater complexity.

Using their spatial resolution, lattice-based approaches can be classified as each lattice site can comprise of a single cell in Cellular Automata (CA) models [12]. Each cell is modified with separate simulation mechanisms at each step: mobilization of cell, proliferation of cell and cell apoptosis. Typically, such methods update the lattice sites to eliminate grid artifacts in a random order.

Models of lattice gas cellular automata (LGCA) may hold more than one cell in each lattice site. LGCA models can model the number of cells moving between individual lattice sites through channels instead of each cell's movement. They can effectively simulate huge number of cells over long periods of time.

Other lattice based modeling technique is cellular pots model (CPM) that holds multiple lattice sites for individual cell in order to enhance the resolution of output and cell morphology in the simulation model[13]. Even though CPM models can give better simulation outputs than other lattice-based models, they require more computational

power.

In off lattice models, cells are symbolized by the individual particulate or mass of many particulates which may ceaselessly migrate in free space. Off lattice models can be mainly classified as center-based models (CBM) that mainly center on masses and volumes on the cells, and boundary-tracking models which use the cell boundaries. These modelling methods can be also classified according to cell morphologies.

In CBMs, centers of cell volume and cell mass can be modeled by performing separate software agent for each cell. Certain CBM models sometimes can model cells as points. However, most of the CBM models simulate cells using their mass and volumes. Moreover, cells are computed and positioned using their physical forces which are adhesive, repulsive, locomotive and drag like forces in order to simulate the growth during the process of time in CBM models [13]. CBM models also are able to simulate the tumor growth not only spheroid shapes but also ellipsoid or nonuniform structures to obtain more realistic simulation outputs. In summary, cells can be simulated using mechanical and rule dependent movements as clusters or nonuniform structures in order to represent the tumor growth by showing the cell morphology in detail with more computational complexity and cost.

Boundary tracking models are comprised of vertex based and front tracking models. These models are suitable for simulation especially fluent tissues. The physical forces that act upon the cell corners including junction points can be computed in vertex-based models. In front tracking models, edge and borders of cell clusters can be modeled with greater spatial resolution. Boundary tracking methods are the most complex cell-based simulation techniques based on the computational needs.

Comparison of lattice free and off lattice based models are illustrated below Figure 2.4 [14].

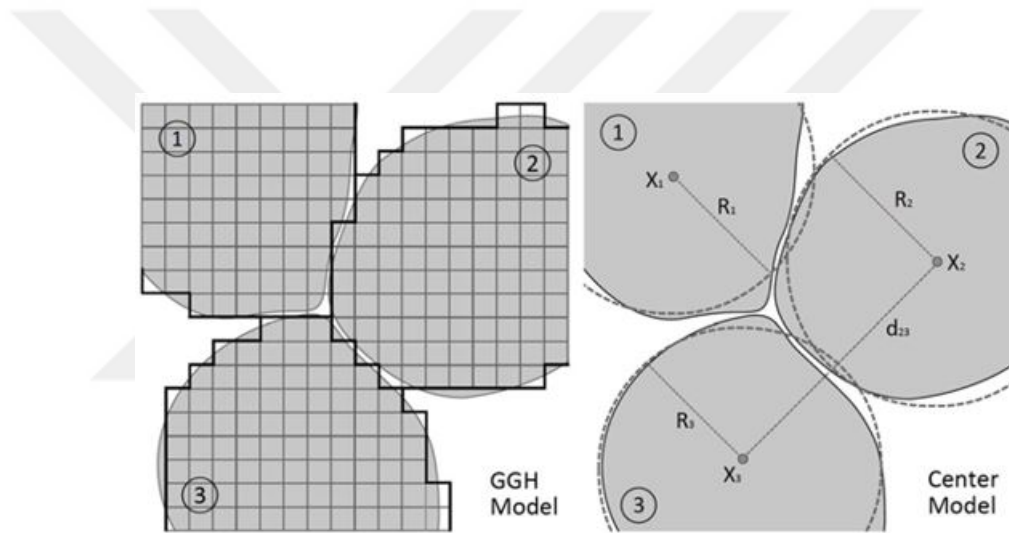


Figure 2.4 Illustration of lattice based(left) and off lattice based(right) simulation models.

3. LITERATURE SEARCH

3.1 Open Source Softwares for Tumor Growth Simulations in the Literature

We analyzed each open source software currently used by researchers in their studies considering inputs and outputs of the softwares and also showing their weaknesses and strengths.

Chaste (Cancer, Heart and Soft Tissue Environment) is the one of the main open source softwares for tumor modelling. Many modelling techniques which are Cellular Automata (CA), Cellular Potts Model and Center-based models can be run together with Chaste simulation environment. Hence, Chaste is capable to simulate both lattice based and off lattice based models with an application program interface. Currently, Chaste only can be used with Linux or Linux system that can be host by Windows or MacOSX. Chaste provides libraries which are common cell mechanisms such as cell proliferation, cell signaling and the nutrient and oxygen transfers from the environment for code which is common to many computational biology problems. One of the examples using Chaste is the oxygen transfer between cell and environment in a growing tumor spheroid as shown in Figure 3.1 [15]. Other example is the development of intestinal crypts (including intestinal crypt geometry, Wnt signaling pathway and intestinal cell cycle) during the initiation of colorectal cancer [16]. Chaste has several advantages such as having own library, using with PDE and ODE and also implementation capability of the lattice based and off lattice-based models. However, it is a Linux based software and it is not easy to use program for the starters for the version that is before 3.2.

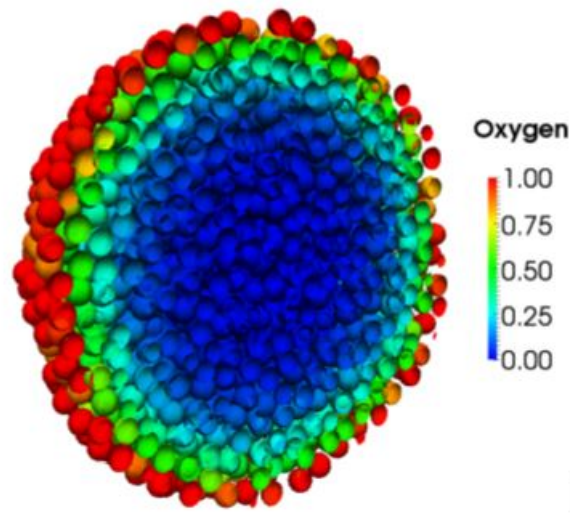


Figure 3.1 Oxygen Concentration in the Growing Tumor Spheroid.

Netlogo is the agent based simulation tool created by Uri Wilensky and William Rand. Cellular automata (CA) and lattice gas cellular automata (LGCA) can be implemented into the Netlogo simulation tool. Besides lattice-based models, off lattice models were implemented to compare the model methods during tumor progression and cell & extracellular matrix adhesion in a specific study. In Netlogo, tumor growth can be simulated using the elements from Wilensky's tumor model in the library. The software can create a place that can be changed the inputs affect the tumor growth, vascularization and immune response. In the Wilensky's tumor model, tumor cells are allowed to divide, move or die depending on nutrition consumption and immune cells quantity between the lattice sites as shown in Figure 3.2 [17]. Netlogo model works using Java Platform that limits the execution environment and cause the performance loss with high number of metastatic cell during the tumor proliferation.

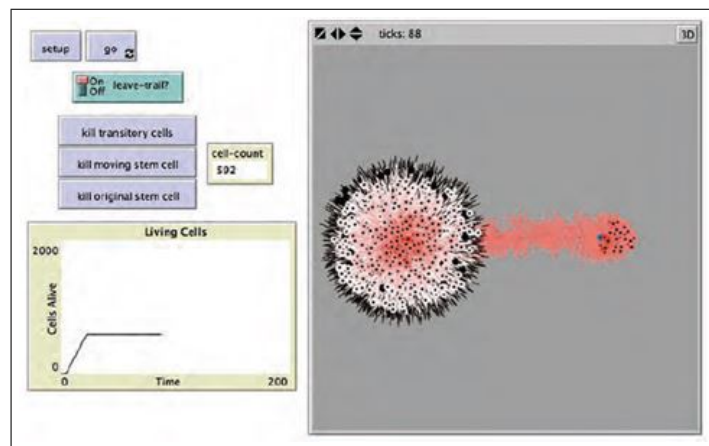


Figure 3.2 Wilensky's Tumor Model in Netlogo.

Recursive Porous Agent Simulation Toolkit (Repast) is also a platform based on Java. It is an agent-based modelling toolkit that can implement the cellular automata (CA) as lattice-based technique. Main focus of REPAST software is the social science including network analysis. However, Repast was updated to Repast Symphony that is the more useful tool for biomedicine. Since, it is capable to give visual output for the simulation. An example study using Repast simulates the proliferation of malignant brain tumor triggered by environmental variables, toxic metabolites and nutrient supplies [18]. Repast also used in the immunotherapy studies (effect of the cytotoxic T lymphocyte quantity for nasopharyngeal carcinoma) [19] during the tumor progression as shown in Figure 3.3. Repast is a grid-based simulation toolkit. It causes the grid-based artifacts during the simulation of tumor growth. Repast creates a 2D simulation output in the lattices. However, for the tumor progression, multilayer 3D simulation is more appropriate to simulate the tumor structures.

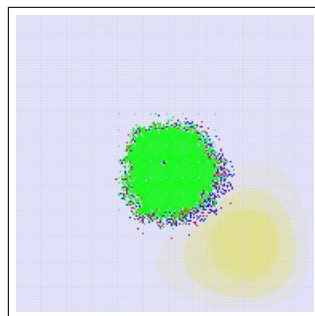


Figure 3.3 Tumor growth simulation in Repast. The green, blue and red dots represents tumor cells and yellow shades shows nutrient concentration.

CompuCell3D has been developed by Maciej Swat. CompuCell3D (CC3D) is another open source software using cellular pots model as lattice-based techniques that is able to simulate 2D and 3D visual output and also vascular and avascular tumor cell proliferation. CompuCell3D creates a tumor simulation environment including virtual-tissue, cell aggregation, cell movement and using the cellular pots models. CompuCell3D provides partial differential equation solvers that can implement the simulation with biochemical reactions and networks. CC3D also create a simulation environment using subcellular signal networks and metabolic activities with the help of System biology markup language (SBML). Hence, CC3D is a software that can simulate the cell and tissue level activities creating a biological environment. Python scripts can be implemented the simulation model in CC3D for especially macro continuum models. In the tumor growth simulations, cell adhesion, glucose concentration, nutrient concentration and cell proliferation phases and also angiogenesis factor for vascular and avascular developments can be used as the inputs for the simulation as illustrated in Figure 3.4 and Figure 3.5 [20] [21]. Cell adhesion features to extracellular matrix during the tumor invasion of ovarion cancer was simulated in CC3D [22]. In another 2D lattice based study in compucell3D, ductal carcinoma in situ (DCIS) was simulated considering four different morphologies (cribroform, comedo, micropapillary and solid) with the inputs that are cell proliferation, apoptosis, necrosis, contractility and adhesion. Cell-cell adhesion in tumor growth has been also simulated using intracellular E-cadherin and β -catenin dynamics in the tumor growth [23]. CC3D is one of the most commons open software for the tumor growth simulation. However, CC3D runs with cellular pots model with lattice based technique that causes the grid based artifacts during the tumor simulation. CompuCell3D benefits the its multiple processors that are comprised of different units like memory graphical processors. The current format of CompuCell3D may run more than 10^7 cells in a week.

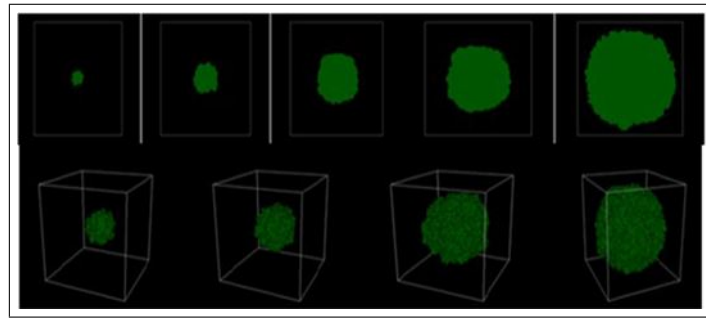


Figure 3.4 Avascular cell proliferation in two dimensional (upper part) and three dimensional.

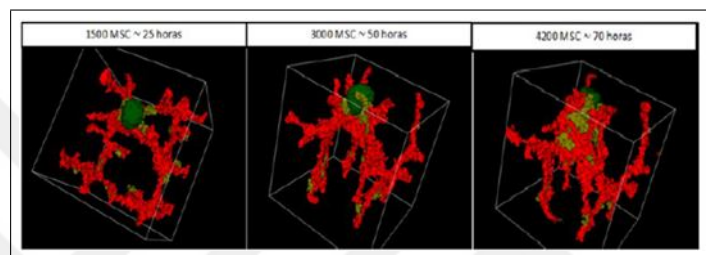


Figure 3.5 Vascular 3D model of stem cells. Green section represents tumor cells. Red parts are blood vessels and yellow parts are new blood vessels.

EPISIM is open software that includes two different sub-software which are EPISIM modeler and EPISIM simulator. SBML models can be implemented to the software with EPISIM modeler. That models are transformed a 2D and 3D tissue and cell simulation including tumor simulation with EPISIM Simulator. SBML models can be integrated to the EPISIM software as CompuCell3D. However, EPISIM is more user friendly and it can be used without coding knowledge. Main goal of EPISIM is the community that has no professional compute skills. EPISIM currently is not common software for tumor modelling. However, it has been used for simulation of cell proliferation and tissue simulation[24].

Morpheus is an agent-based simulation software that is used for the cell-based and tissue environment simulations considering reaction-diffusion systems. Cellular pots model (CPM) can be implemented for tumor proliferation and growth considering oxygen consumption, nutrient concentration and the cell life cycles. Morpheus has a graphical user interface for the alteration of parameters and the image output of the simulation. It is also used with partial and ordinary differential equations combining

with cellular pots model in the hybrid studies such as vascular network formation by paracrine signaling [25]. Morpheus is a multi-scaling simulation software that can be combined PDEs/ODEs, cellular pots model, reaction-diffusion systems and also SBMLs. Hence, for the multi scaling simulations and hybrid studies, Morpheus can be good option for the simulation.

Tissue simulation toolkit is a lattice-based simulation software which can be implemented the cellular potts model created by Graner and Glazier. Growth mechanism of cell and tissue can be simulated in the tissue simulation toolkit with two-dimensional simulation output. Tissue simulation toolkit first described by R M H Merks, J A Glazier [26]. In the study that is the center-based approach of developmental biology. Tissue simulation toolkit works with the help of C++. Hence, Basic knowledge of C++ is necessary to use tissue simulation kits. Vascular structure, tumor angiogenesis and cell mechanisms and cell movements can be simulated via tissue simulation toolkit integrating cellular pots model and partial differential equations [27]. Tissue simulation toolkit is only capable to simulate two dimensional structures and requires basic computation background before using it.

Biocellion is a center based off lattice model simulation software that is capable to simulate very high number of cells and tissue environment using the parallel computers in the same time. Biocellion is one of the main softwares without restrict the simulation model with agents and lattice sites [28]. Biocellion can run very fast the recurrent source codes (diffusion concentration, cell proliferation and etc.) in the model with the integration of algorithms developed by high-performance computing (HPC) community. Main goal of Biocellion is to simulate the cells that have number more than 10^9 . Biocellion has three different substructure that can be coded as cell states, cell to cell interactions and cell to ECM interactions. Biocellion users can simulate their work in the personal computer and they can upload the code in the cloud system for integration with other computers to achieve faster modelling performance. Biocellion cannot provide a cell represented by many lattice sites and this causes less resolution in the cell shape and less details of interactions between the cells. Biocellion provides the partial and ordinary differential equation solver for cell proliferation and

tissue simulation in the software but for the other equations like regulations of cell, users should implement to the their equation solver using specific approaches and this cause more time for programming. Hence, Basic C++ knowledge and mathematical background is necessary for using the software. Biocellion also cannot simulate the all environmental conditions such as blood flow and water flow modelling. However, cell shape resolution and three-dimensional simulation outputs gives more consistent data than the two-dimensional lattice-based models. biocellion is a good area for the complex system simulations such as tissue growth, tumor proliferation including environmental factors. An example study states that simulation of skin. Skin is very complex biological sub structures in the epidermal growth and it is simulated using Biocellion integrating discrete agent-based modelling, ordinary and partial differential equations [29].

FLAME is an off-lattice technique simulation software. Center based model can be implemented to FLAME software. FLAME is not an exact simulation tool. Since, FLAME creates the codes that are necessary for the modelling and simulation platform. Simulation codes are created in C language. Hence, basic software background is must for running of FLAME and the related simulations. FLAME can be used with parallel softwares in order to achieve better performance during the simulation. Three-dimensional simulation can be created in FLAME such as epidermis considering cell cycles, cell differentiation rules and also physical forcings including displacement of each cell, adhesive forces [30]. Moreover, multi scale tumor growth in Colorectal cancer can be simulated using tissue vascularization, interaction between the cells, cell proliferation and vascular endothelial growth factors through the oxygen consumption and VEGF concentration as represented in Figure 3.6 [31]. An important disadvantage to the FLAME simulator is that the movement of cells between process cannot be modeled. This results in evolution of the initial population being the determinant of the workload of each process.

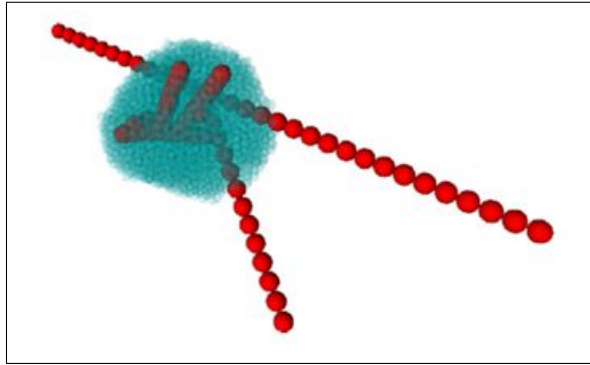


Figure 3.6 Tumor simulation in FLAME. Blue colors represent tumor cells and red dots represent blood vessels.

Physicell is a three dimensional and center based simulator using off lattice model rules including general cell proliferation rules such as cell cycle, apoptosis, necrosis and also physicell has an advantage over the other agent based models creating simulation environment considering fluid dynamics of cell, cell secretion substances, mechanics and motility of cells, cell volume and the physical forces of cells such as adhesion and repulsive forces [32]. Physicell is a lattice free simulator software. Hence, it reduces as much as possible simulation artifacts caused by lattice or grid sites. In this simulator, millions of cells can be simulated up to 10^6 cells solving the many partial differential equations in the same time that differs from the other softwares that generally solves one PDE at a time. Essentials of cell proliferation such as proliferation, apoptosis and etc. have already been embedded to Physicell. Hence, user can focus mostly other parameters of tumor growth or cancer progression such as environmental issues, physical forces, tissue/cell vascularization (angiogenesis) and cell - environment determinants instead of losing their times for programming the essentials of cell proliferation. Immunity and tumor heterogeneity can be simulated during the tumor growth and cancer progression in Physicell as well. Ductal carcinoma in situ (DCIS), glioma growth, anti-cancer nanorobots and vascular tumor growth can be simulated in Physicell as well. There is no sample code for implementation of extracellular matrix during the simulation in Physicell. Hence, user can implement their ECM models for the simulation arrange the positions of cell in the model. And also, Physicell is not a good option to simulate the morphologies of cell. For the morphology related studies, users can implement the elongated cells to more than one agent in the Physicell designing

adhesive connection between the cells. Moreover, SBML is not compatible with Physi-cell. Hence, users cannot implement the SBML to their simulation model to vary the cell shapes.

Timothy is an off lattice and center-based simulation software that can integrate partial and ordinary differential equations in the continuous and dynamic system which are the intracellular and extracellular modelling. Timothy has been designed to simulate the number of cells more than 10^9 using super computers. Hence, Timothy is capable to simulate the cellular level, sub cellular and tissue level activities in one model. Cellular level activities such as cell cycles phases interact with the continuous environment system to create multi scale simulation model. Tumor growth and its biological complexity can be simulated in Timothy using cell phases, nutrient and oxygen concentration in intracellular and extracellular matrix and also considering the extracellular matrix fibrous and collagen structures [33]. Large scale simulation capability of Timothy has the main advantage over the other agent-based simulations to create a tissue level simulation model. However, Timothy's large-scale simulation capability also causes a disadvantage because of the very complex computational need.

4. METHODS

4.1 Comparison Method and Search Strategies for Open Source Tumor modeling Softwares

The open source softwares that have been used for the tumor modeling and tumor progression related studies have been searched. Based on the literature findings, the specific area for the progression of cancer that is used in each software has been defined to make a concrete guide for the programmer to select most appropriate open softwares related with their research field.

Comparison of softwares have been determined based on four main features.

First of all, the applicable methods for the open softwares have been listed. Hence, preferred agent-based methods which are lattice based or off lattice based can be selected considering pros and cons of these two methods [11] [13]. Since, lattice structure of software is one of the important features that affects the simulation output in terms of grid-based artifacts [9].

Secondly, integrated approaches that are cellular automata, center-based and vertex approaches of the softwares were examined. These approaches determine how many cells each agent holds in the simulation environment. And these approaches have direct effect on the simulation output in terms of resolution, dimension [11].

Thirdly, inputs of each software that were integrated in the studies have been specified according to literature search. Each software structure has different features based on implantation of inputs that are cell progression, intratumor heterogeneity, the microenvironment factors etc. And the softwares should be selected based on the inputs that will be investigated during the tumor progression.

Lastly, output features of each softwares have been criticized. Since, each software gives different outputs based on their programmable structure such as two-dimensional or three-dimensional simulation data and vascular or avascular outputs. Softwares should be selected based on the output that is aimed to analyze end of the simulation [13].

4.2 Integration of Models for Diagnosis and Prediction of Cancer Treatment

Tumor removal often leaves cancer cells left over from the operation which can regrow and metastasize to other areas. Enderling et al. [3] used agent-based model (ABM) to study relapse following surgical removal and observed that residual cells from tumor removal often result in tumor relapse and the tumor progresses along the mutation pathway. However, adjuvant radiation therapy after surgical excision showed to high chance of reducing secondary tumor formation and killing residual cancer cells.

Powathil et al. [34] used a hybrid multiscale ABM to study how chemotherapy and hypoxia affect the tumor microenvironment. Their model included the cell cycle stage and used an approach developed by Tyson and Novak (insert citation) which uses ODEs to calculate how the concentration of five key mammalian proteins and the cell mass changes across the cell cycle. This method allowed them to look at how different chemotherapy agents were effective in different stages of the cell cycle since many chemotherapy drugs work by interrupting a specific stage of the cell cycle and looking at how hypoxia can reduce cellular division and inhibit treatment using chemotherapy drugs. They observed that limitations in oxygen diffusion mentioned before in the discussion of the necrotic core, result in heterogeneity in HIF-1 α across the tumor. This difference in HIF-1 α concentration leads to cells at different stages of the cell cycle in the tumor and thus the drug kills cells at different effectiveness across the tumor. Further understanding of the dynamics of the redistribution of oxygen and cell growth can allow for better optimization of timing between treatment and advance

effort towards patient-specific treatment.

ABM has also been used to improve anti-cancer vaccine efficacy by looking at how the immune system responds to different tumors. Particularly, researchers have looked at how to prime cytotoxic T lymphocytes against new tumors before a clinical diagnosis. A hybrid ABM simulates wet-lab experiments to predict the minimum number of vaccinations required to prevent lung metastases in vivo. Much of this research focuses on detailed modeling of the immune response to understand what is going on in vivo. For example, Preissner et al. [35] have developed different ABMs which model real amino acid sequences of immune receptors and their ligands to see the in silico response of a peptide vaccine in cancer immunotherapy with a better capability to predict real-life events.

4.3 Tumor Growth Simulation in PhysiCell v1.6.1

Among the simulation softwares listed in Table xxx, Physicell v1.6.1 has been used to simulate the tumor growth including cell cycle and tissue microenvironment parameters. Physicell is an open source program that uses C++ platform with the integration of Matlab and Paraview codes. Physicell also has its own differential equation (PDE/ODE) solver (BioFVM) for biotransport equations (diffusion and secretion of nutrient). Physicell has already integrated basic cell functions (cell cycles, cell adhesive/repulsive forces, cell apoptosis and necrosis states) apart from the other simulation platforms. Hence, users can easily change the tumor growth inputs without writing new codes in C++ platform. Most of the simulation platforms solve one PDE at each time step and this causes more time to simulate 3D tumor structure comparing with Physicell. Physicell can solve many differential equations in the same time to reduce the simulation time in order to achieve the tumor structure that comprises 10^5 and 10^6 cells.

Matlab R2016b has been used for plotting of chemical substrates in the tumor microenvironment with the integration of Physicell outputs as .XML format.

Paraview v5.4.1 has been used for the 3D Animated Tumor Growth with the help of Phyton 2.7.16 script codes.

4.4 Physicell v1.6.1 Working Principle and Software Features

PhysiCell is a software that simulates the interactions and dynamics of cells in 3-D microenvironments with the phenotype dependent on the environment [32]. PhysiCell's lattice-free physics-based approach reduces grid-based artifacts and provides optimized, biologically accurate functions for key cell behaviors. So, the user can simulate cell behaviors such as cell cycling, cell death, volume/biomass control, motility, and mechanical interactions between cells through defined functions. PhysiCell builds cell agents with a hierarchical phenotype data structure. The phenotype data is modified by the simulator to regulate (trigger and control) phenotypic processes so users don't have to these processes and can concentrate on designing microenvironment dependent triggers of cell processes. PhysiCell's modular code still allows users to modify or replace default functions or create rules to assign to specific agents. PhysiCell is also fully integrated with a fast multi-substrate diffusion code called BioFVM that can solve for vectors of diffusing substrates. This integration allows users to tie cell phenotype to different diffusing signals.

Simulation is managed by three different time steps as described below;

- `diffusion_dt`: Substrate concentration rate in the microenvironment is followed with the step size `diffusion_dt`. The default constant is 0.01 min.
- `mechanics_dt`: Cell motility is followed with the step size `mechanics_dt`. On this time period, custom fuctions are speciliazed for each cell are also determined. The default constant is 0.1 min.
- `phenotype_dt`: Phenotypic features including basic cell behaviors are maintained with the step size `phenotype_dt`. The default constant is 6 min

Physicell can be run with the one of the C++11 compilers with OpenMP support. In order to run Physicell in Microsoft Windows operating system, MinGW-w64 via g++ should be run on the computer as a compiler. Physicell codes can be worked in the parallel computers via OpenMP to simulate up to 10^6 cells on the desktop computer or more than 10^6 cells with the super computers.

4.5 Overall Simulation Working Principle

In PhysiCell, t_{mech} (cell mechanics features are worked at the following time), t_{cells} (cell processes are worked at the following time) and t_{save} (following simulation output time) are followed internally with the output rate of period Δt_{save} after starting BioFVM as a microenvironment diffusion solver and cells. PhysiCell is established at the beginning;

$$t_{mech} = \Delta t_{mech}; t_{cells} = \Delta t_{cells}; t_{save} = 0.0.$$

1. The simulation status is kept if $t \geq t_{save}$. Set $t_{save} = t_{save} + \Delta t_{save}$.
2. For the cell agents in the simulation environment, activate the BioFVM for the saturation and diffusion of substrates in the microenvironment
3. After initializing of BioFVM for chemical substrate areas, activate the defined cell process for the current cells in the simulation environment if $t \geq t_{cells}$:
 - Run the defined cell parameters and update their defined phenotype
 - Run the defined cell cycle model and death model for each cell in the simulation environment
 - Arrange the cell volumes including cytoplasm and nucleus volumes in the fixed cell agents in the simulation environment
 - And then arrange $t_{cells} = t_{cells} + \Delta t_{cells}$

4. If $t \geq t_{mech}$, and then:
 - Arrange the cell motility and cell velocity depending on the adhesive and repulsive forces.
 - Each cell agent is updated with the interaction of the force-based velocities and motilities via Adams-Bashforth method.
 - Arrange $t_{mech} = t_{mech} + \Delta t_{mech}$
5. Latest and ongoing simulation time is updated by $t = t + \Delta t_{diff}$. And then, return to Step 1.

4.6 Biochemical Microenvironment

A vector of diffusion-reaction partial differential equations (PDEs) related with diffusion and decay rates are used in the BioFVM to simulate the microenvironment for chemical reactions [36]. The biochemical microenvironment (discretized as a Cartesian mesh (Ω) for computational efficiency) is modelled as a vector of reaction-diffusion PDEs for a vector of chemical substrates ρ of the form as;

$$\partial\rho/\partial t = D\nabla^2\rho - \lambda\rho \quad \text{in } \Omega \quad (4.1)$$

Where D and λ are the vectors of diffusion coefficients and decay rates,

To solve the vector of diffusion-decay PDEs, BioFVM use the locally one-dimensional (LOD) method: a specialized operator splitting that turns the 3-D PDEs into a sequence of one-dimensional PDEs.

4.7 Cell Volume

Overall cell volume is defined as V (total cell volume) that is comprised of fluid and solid biomass volumes respectively as V_F and V_S . Solid biomass volume also has sub-volumes which are nuclear solids (V_{NS}) and cytoplasm solids (V_{CS}) that represent cell nucleus and organelles. Apart from the overall cell volume, cell's main sections are defined as total nuclear volume (V_N) and total cytoplasm volume (V_C) that includes all fluid and solids in the nucleus and cytoplasm. All these mentioned volumes in the cell structure are modelled with a basic ordinary differential equation as below [32];

$$\frac{dV_F}{dt} = r_F(V_F^*(t) - V_F) \quad (4.2)$$

$$\frac{dV_{NS}}{dt} = r_N(V_{NS}^*(t) - V_{NS}) \quad (4.3)$$

$$\frac{dV_{CS}}{dt} = r_C(V_{CS}^*(t) - V_{CS}) \quad (4.4)$$

where r_F , r_N and r_C are rate constants, and V_F^* , V_{NS}^* and V_{CS}^* are the aim volumes.

Based on the equations given above. Reference parameters are calculated as Table 4.1 below [8] [37]. These volumes are calculated through each cell cycle and cell death functions.

Table 4.1
Reference Parameters for Cell Volume.

Parameter	Biophysical Description	Reference Value
V	Overall cell volume	$1670 \mu m^3$
V_N	Overall nuclear volume	$465.76 \mu m^3$
V_C	Overall cytoplasm volume	$1204.2 \mu m^3$
r_F	Rate of water exchange	3.0 hour^{-1}
r_C	Rate of cytoplasmic solid biomass	0.27 hour^{-1}
r_N	Rate of nuclear biomass	0.33 hour^{-1}
V_{NS}^*	aim nuclear solid volume	$135 \mu m^3$
f_{CN}	aim cytoplasmic: nuclear volume fraction	3.6
f_F	aim water ratio	0.75

4.8 Cell Cycle General Rule

Cell proliferation is combination of phases in the cell cycle model $\{X_1, \dots, X_n\}$ and its transition rates $\{r_{ij}\}_{i,j=1}^n$ between the phases, where r_{ij} is the transition rate from the i^{th} phase to the j^{th} phase. In some certain cell cycling phases, total cell volume and sub-volumes are also altered. Each cell agent (k) in the simulation model has own phenotypic phase $S_k(t) \in \{X_i\}_{i=1}^n$ and the total time spent (t_k) in cell agent's current phase. In any time interim $[t, t + \Delta t]$ a cell with $S_k(t) = X_i$ possesses a likelihood of termination the X_i phase and initiation the X_j phase given by

$$Prob(S_k(t, t + t) = X_j | S_k(t) = X_i) = 1 - \exp(-r_{ij}\Delta t) \approx r_{ij}\Delta t \quad (4.5)$$

4.8.1 Cell Division

Cell cycle model is the main element of cell proliferation. general rules are occurred respectively as below when a cell agent k divides;

1. Sub-volumes of cell agent are split in half
2. Readjust the phase time as t_k to 0
3. Double the cell (including all related cell parameters)
4. Locate the cell and its double

4.8.2 Flow Cytometry Separated Cell Cycle Model

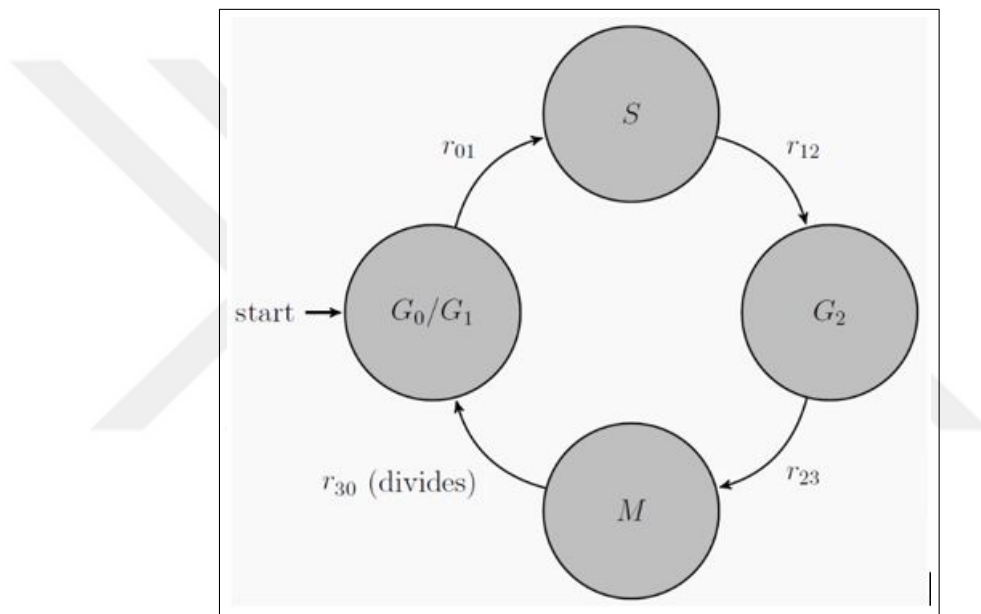


Figure 4.1 Illustration of Flow Cytometry Separated Cell Cycle Model.

In this model as shown in Figure 4.1, $G_0=G_1$ cells can enter the cell cycle to become S-phase cells, at transition rate r_{01} . S-phase cells can become G_2 -phase cells at rate r_{12} . G_2 -phase cells can become M-phase cells at rate r_{23} . M-phase cells can divide into two $G_0=G_1$ daughter cells at rate r_{30} . The population-scale model is given by:

$$\frac{dG_0G_1}{dt} = -r_{01}[G_0G_1] + 2r_{30}[M] \quad (4.6)$$

$$\frac{dS}{dt} = r_{01}[G0G1] - r_{12}[S] \quad (4.7)$$

$$\frac{dG2}{dt} = r_{12}[S] - r_{23}[G2] \quad (4.8)$$

$$\frac{dM}{dt} = r_{23}[G2] - r_{30}[M] \quad (4.9)$$

Based on the equations above, time duration of each phase has been calculated using a simple iterative fitting method in Matlab R2016b as below Table 4.2.

Table 4.2
Cell Cycle Reference Durations.

Parameter	Biophysical Description	Reference Value
T_S	Duration of S phase	8 hours
T_{G2}	Duration of G2 phase	4 hours
T_M	Duration of M Phase	1 hour
T_{G0G1}	Duration of G0G1 Phase	4.98 hours

Overall cell cycle duration for each cell is approximately 18 hours based on the reference values.

4.8.3 Oxygen-dependent phenotype

In order to update the cells proliferation and death parameters based on the oxygen concentration in the microenvironment, oxygen-dependent phenotype model has been developed. In the cancer study, oxygen concentration is one of the key elements that directly affects tumor growth. Oxygen concentration affects both cell proliferation rate and necrosis rate.

4.8.3.1 Overall model for proliferation.

- Sample the microenvironment for the oxygen concentration σ at the cell center.
- If $\sigma \geq [\text{parameters.o2_proliferation_saturation}]$, then the cycle entry rate is set to 100%
- If $\sigma \leq [\text{parameters.o2_proliferation_threshold}]$, then the cycle entry rate is set to 0%

To sum up, cycle entry rate is modelled by;

$$\frac{\sigma - [\text{o2_proliferation_threshold}]}{[\text{o2_proliferation_saturation}] - [\text{o2_proliferation_threshold}]} \quad (4.10)$$

4.8.3.2 Overall model for necrosis.

- Sample the microenvironment for the oxygen concentration σ at the cell center.
- If $\sigma \geq [\text{parameters.o2_necrosis_threshold}]$, then the cycle entry rate is set to zero
- If $\sigma \leq [\text{parameters.o2_necrosis_max}]$, then the cycle entry rate is set to 100%

To sum up, the necrotic death rate is modelled by;

$$\frac{[\text{o2_necrosis_threshold}] - \sigma}{[\text{o2_necrosis_threshold}] - [\text{o2_necrosis_max}]} \quad (4.11)$$

Reference oxygen parameters that have been used in the model listed as below:

Table 4.3
Oxygen Dependent Phenotype Reference Values.

Parameter	Reference Value
O_2 Hypoxic Threshold	15.0 mmHg
O_2 Hypoxic Response	8.0 mmHg
O_2 Hypoxic Saturation	4.0 mmHg
O_2 Necrosis Threshold	5.0 mmHg
O_2 Proliferation Threshold	5.0 mmHg
O_2 Proliferation Saturation	38 mmHg
O_2 Reference	160 mmHg

4.9 Cell Coloring in Simulation Output

PhysiCell v1.6.1 can simulate transmitted light microscopy to create virtual HE (hematoxylin and eosin) images, as well as false-colored images. These images are saved as SVG (scalable vector graphics) files, which allow lossless rescaling of the image.

Colors in SVG files can be specified as RGB colors that are a string of the form "rgb(R,G,B)", where R, G, and B are the red, green, and blue values, and they are integers between 0 and 255. Coloring of flow cytometry cell cycling model is specified as shown in the Table 4.4.

Table 4.4
Coloring of SVG outputs for each cell type in the Tumor Structure.

Phase	Color
G0/G1 cells, or G1 cells	light blue (0,80,255)
G0 cells	pale blue (40,200,255)
S cells	magenta (255,0,255)
G2 cells	yellow (255,255,0)
G2/M and M cells	green (0,255,0)
apoptotic cells	red (255,0,0)
necrotic cells	brown (250,138,38)

4.10 Evaluation Method

Physicell simulation gives visual outputs as svg file format during the simulation. These svg files includes simulation time, real time and number of cells in the simulation microenvironment as two-dimensional images at z axis 0. These outputs also demonstrate each cell stage described in Table 4.4 in the microenvironment. According to svg format visual outputs, tumor growth rate, maximum tumor diameter and necrotic core were interpreted. Tumor growth rate also interpreted via Excel using the number of cells every 360 minutes. Scatter chart has been created for the data with its trendline. Polynomial trendline was fitted our data set with cubic order.

Physicell simulation also create xml file format that is matrix-based structure includes the distribution of substances in the microenvironment and also the distribution of cells in the microenvironment based on the substance concentration. Using these xml files, oxygen concentration in the microenvironment and cell stage in that oxygen concentration were evaluated and understood the correlation between initial oxygen concentration and cell stages. The oxygen concentration in the microenvironment during the simulation also has been demonstrated as oxygen contour plot in the Matlab using the xml files.

5. RESULTS

5.1 Comparison of Open Source Software based on Literature Research

Eleven open source simulation models have been compared based on their input and outputs as described in Table 5.1.

Lattice based models including cellular automata, lattice gas cellular automata and cellular potts models are generally use cell cycles and nutrient/oxygen consumption to simulate the tumor growth with a more limited resolution. Cellular potts models are suitable for three dimensional simulations to represent better cell morphology. CompuCell3D is the most complex cellular potts model, and it uses cell cycles, cell-cell, cell-ECM interaction, and intracellular dynamics as simulation inputs and gives more detailed outputs that show tissue vascularization and tumor growth as three-dimensional with greater computational complexity.

Center based model is one of the common off lattice-based models. Off lattice models are predominantly compute the physical forces between the cells as inputs besides the cell proliferation and intracellular dynamics. Cells can easily move in the free space and provides more realistic outputs based on tumor morphology. Physicell and Biocellion are the most complex simulation toolkits that can simulates the cells over 10^6 using super computers. Simulation of high number of cells shows more realistic tumor structure and cancer progression simulations. They can compute lots of equations at the same time to accelerate the simulation studies. These simulation toolkits possess their own library including essential cell mechanisms such as proliferation. Hence, researchers can focus on the other variables instead of wasting time with programming well known cell growth mechanisms. Detailed comparison table including all simulation toolkits mentioned in method section has been prepared to show all variables carefully considering their biological inputs and their respective output capabilities as below.

Table 5.1
Comparison of Open Source Software Considering Their Inputs and Outputs.

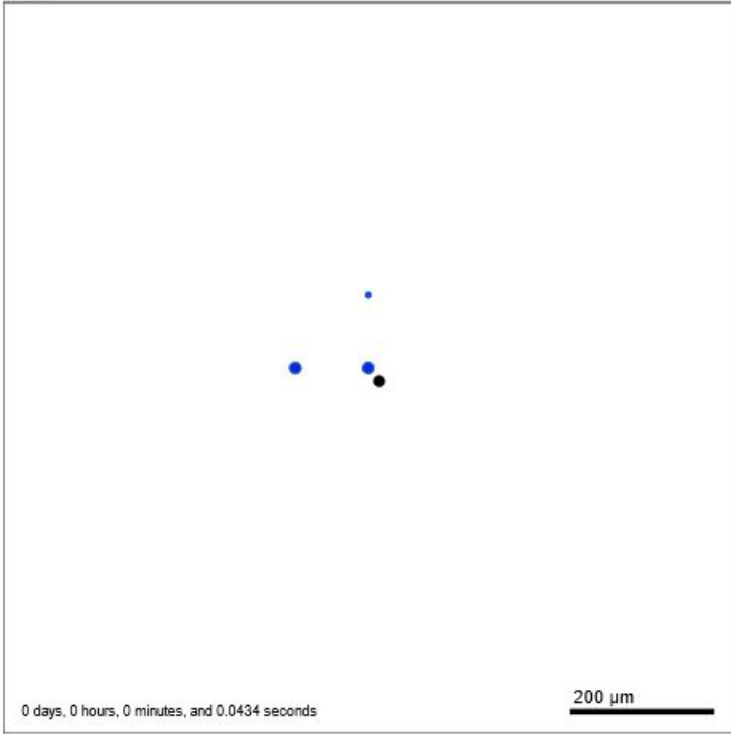
Software	Method	Approach	Inputs	Outputs
Chaste	-Lattice based -Off lattice based	-Cellular Automata -Vertex based -Center based	-Cell cycle -Intracellular signaling pathways -Exchange of oxygen and nutrients -Cell adhesion and migration -Wnt dependent cell proliferation	-2D or 3D Tumor Growth -Tumor and Cell Morphology -Tumor and Cell Angiogenesis
Netlogo	-Lattice based -Off lattice based	-Cellular Automata -Lattice Gas Cellular Automata	-Cell life cycle -Cell proliferation -Exchange of oxygen and nutrients	-2D Avascular Tumor Growth
Repast	-Lattice based	-Cellular Automata	-Cell life cycle -Cell proliferation -Exchange of oxygen and nutrients -Number of immune cells	-2D Avascular Tumor Growth
CompuCell	-Lattice based	-Cellular Potts	-Cell proliferation -Exchange of oxygen and nutrients -Intracellular dynamics -Cell-Cell Adhesion -Cell-ECM Adhesion -Cell Motility	-2D or 3D Tumor Growth -Vascular or Avascular Tumor Growth -Tumor Evolution
EPISIM	-Lattice based	-Cellular Potts -Center based	-Cell life cycle -Cell differentiation -Exchange of oxygen and nutrients -Homeostasis -SBML models	-2D or 3D Avascular Tumor Growth -Cell and Tumor Morphology -3D Tissue Integrity (Epidermal Homeostasis)

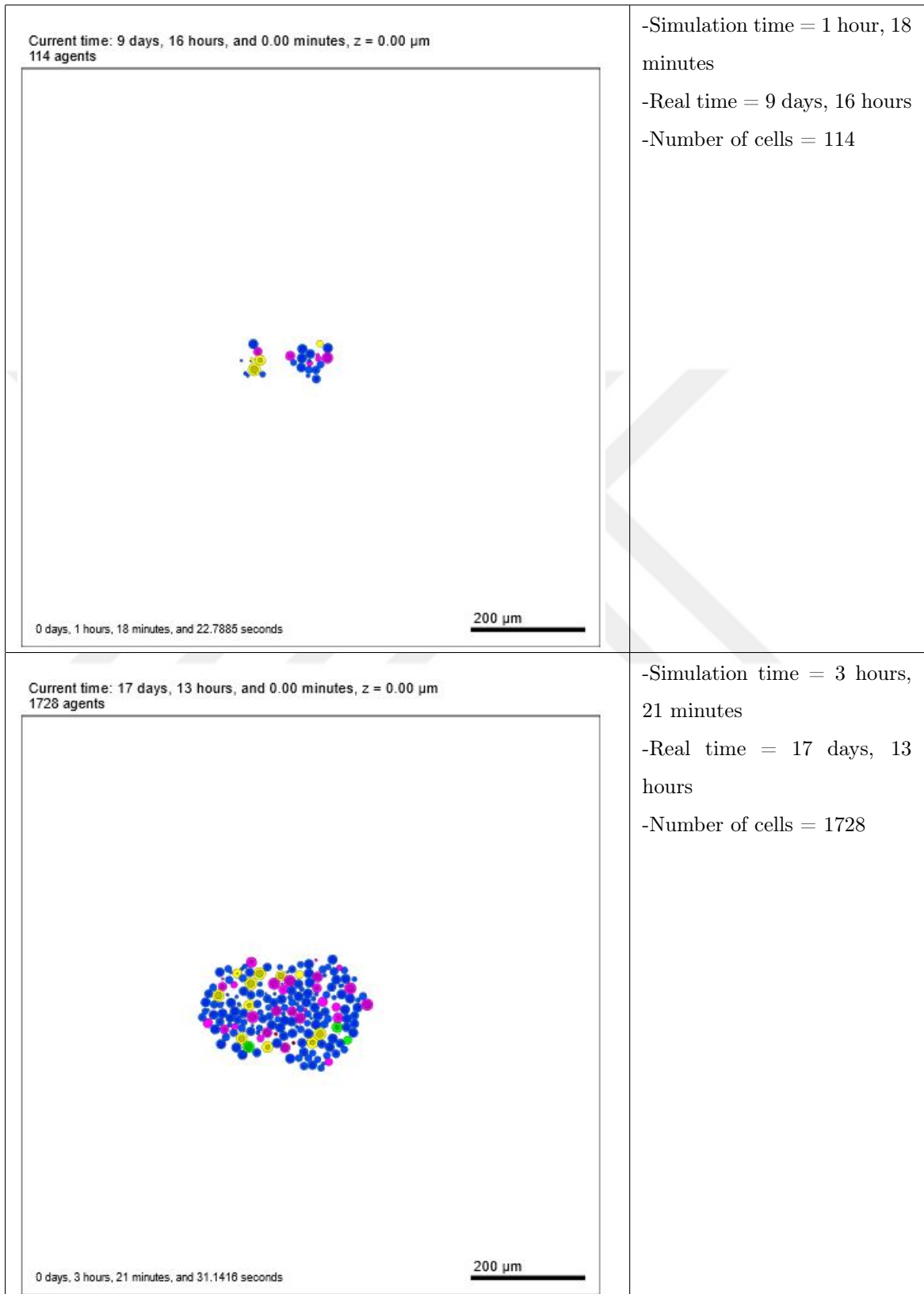
Morpheus	-Lattice based	-Cellular Potts	-Cell life cycle -ReactionDiffusion systems -Cell signaling -Cell adhesion -Biophysical forces of cell	-2D/3D Avascular/Vascular Tumor Growth -Vascular Morphogenesis -Cell Polarization and Chemotaxis
Tissue Simulation Toolkit	-Lattice based	-Cellular Potts	-Cell life cycle -Chemotaxis, haptotaxis and haptokinesis -Cell signaling -Cell adhesion -Biophysical forces of cell -Cell elongation	-2D Vascular Tumor Growth -Vascular Network -Tumor Angiogenesis -Cell motility
Biocellion	-Off Lattice based	-Center based	-Cell life cycle -Glucose consumption -Cell differentiation -Cell mutation -Cell-cell adhesion -Cell-ECM adhesion -Immune Cell Phagocytosis -Blood Vessel Anastomosis	-2D or 3D Avascular Tumor Growth -Cell sorting -Tissue simulation
FLAME	-Off Lattice based	-Center based	-Cell life cycle -Physical forces -Cell differentiation -VEGH concentration -Cell-cell interactions -Cell-ECM adhesion	-3D Vascular Tumor Growth -Tumor Angiogenesis
PhysiCell	-Off Lattice based	-Center based	-Cell life cycle -Cell immunity -Tumor heterogeneity -Physical forces -Cell-cell-ECM interactions	-3D Avascular Tumor Growth -Cell Sorting -Tumor immunity
Timothy	-Off Lattice based	-Center based	-Cell life cycle -Nutrient and oxygen concentration -ECM fibrous and collagen structures -Cell-cell-ECM interactions	-3D Vascular Tumor Growth -Tumor Angiogenesis -Tumor Microenvironment -Tissue Growth

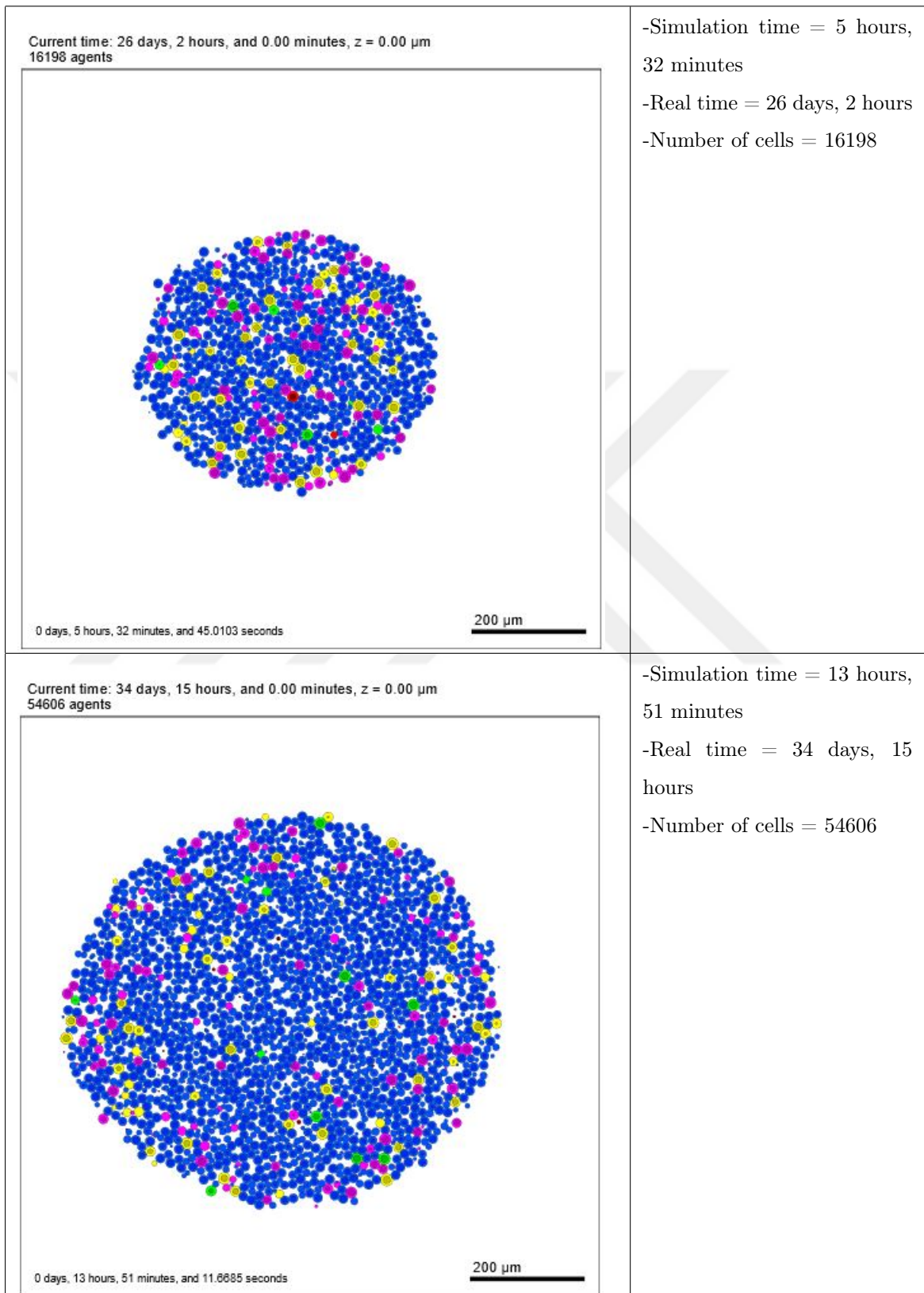
5.2 Tumor Growth Simulation

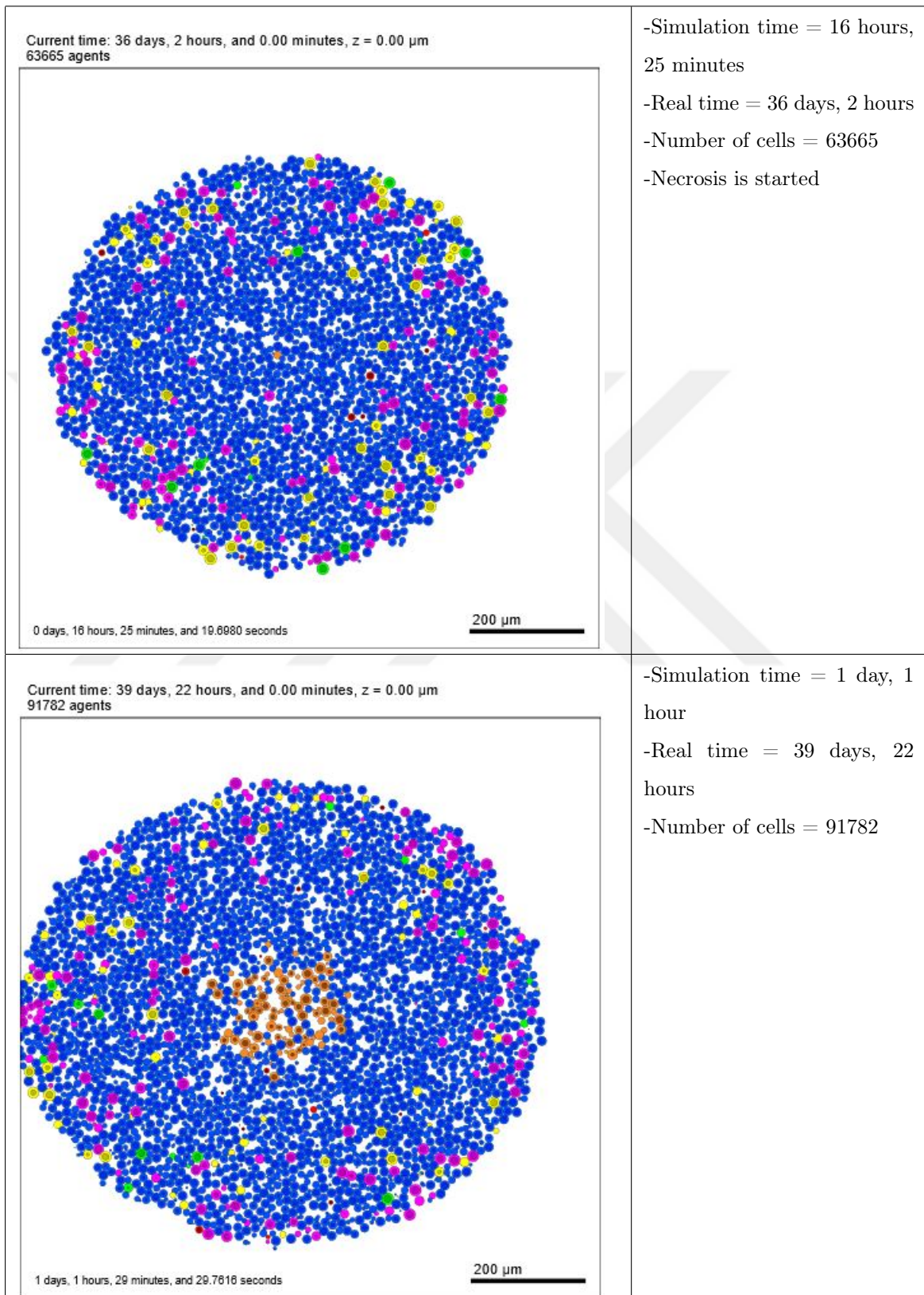
Tumor structure that comprises 150.584 A549 cells has been simulated with the initial substrate is 38 mmHg oxygen as shown in Table 5.2. Cell proliferation has been initiated with four cells using flow cytometry cell cycle model.

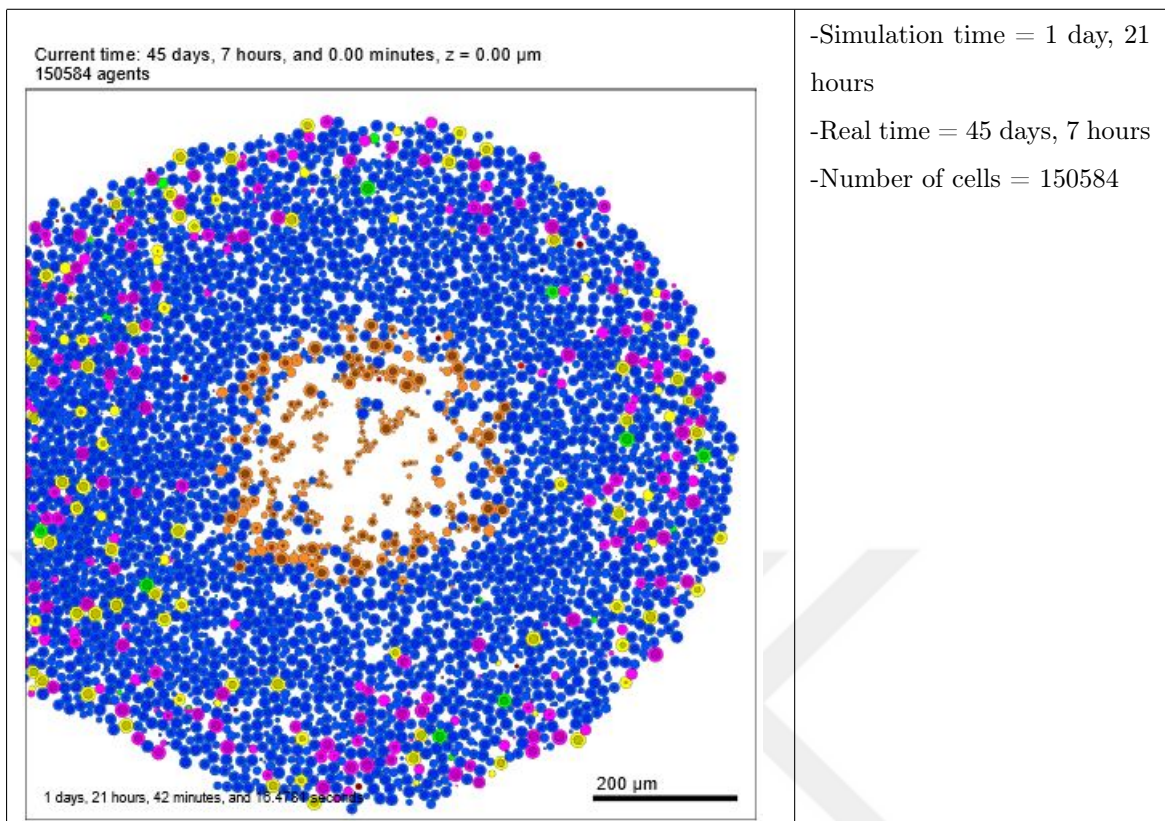
Table 5.2
Tumor Growth That Includes A549 Cells Over Time.

Visual Output of Simulation	Simulation Characteristics (Time, Number of Cells)
<p>Current time: 0 days, 0 hours, and 0.00 minutes, z = 0.00 μm 4 agents</p>  <p>0 days, 0 hours, 0 minutes, and 0.0434 seconds</p> <p>200 μm</p>	<p>-Simulation time = 0 day, 0 minute -Real time = 0 day, 0 minute -Number of cells = 4</p>









Simulation has been completed in 1 day and 21 hours that represents 45 days and 7 hours in real time. Necrosis has been occurred after 16 hours simulation time due to oxygen drop in the tumor microenvironment.

At the end of the simulation with 150584 A549 cells, tumor structure diameter reaches approximately 800 μm with the 400 μm necrosis structure that includes calcified sub-structure. Final simulation output has been visualized using Paraview v5.4.1 as 3D model in below Figure 5.1.

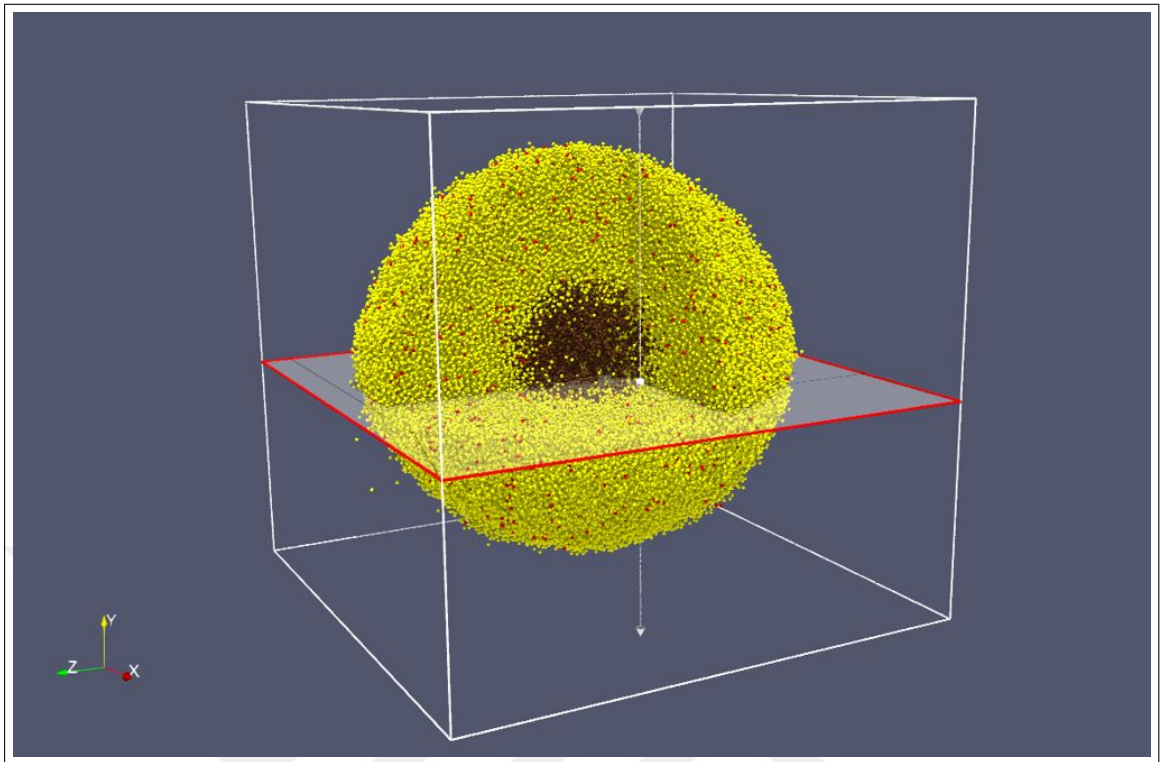
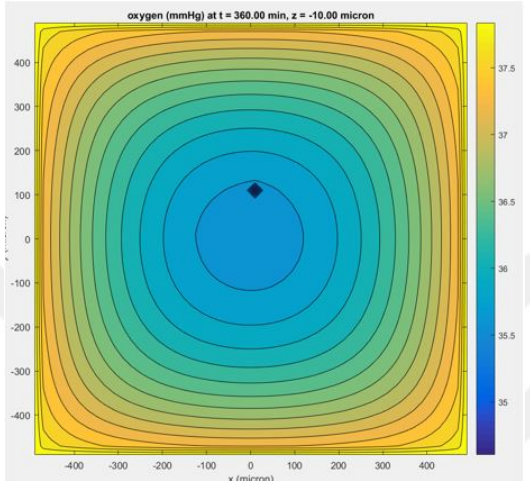
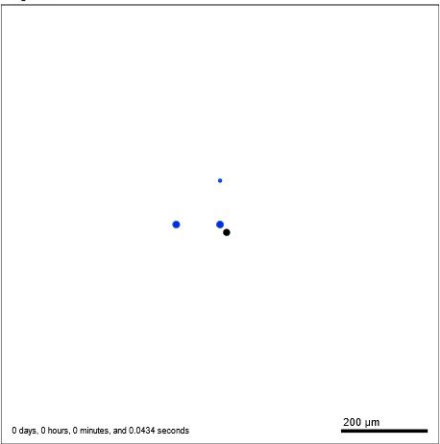
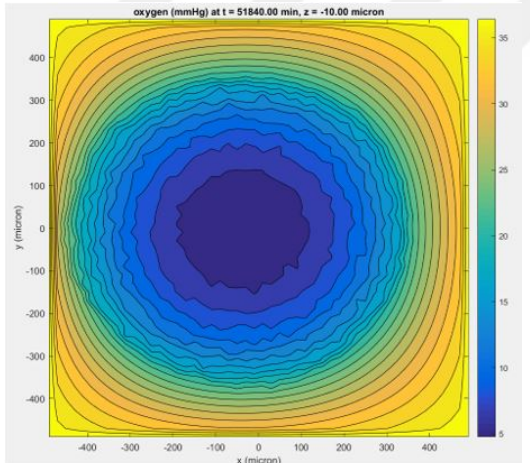
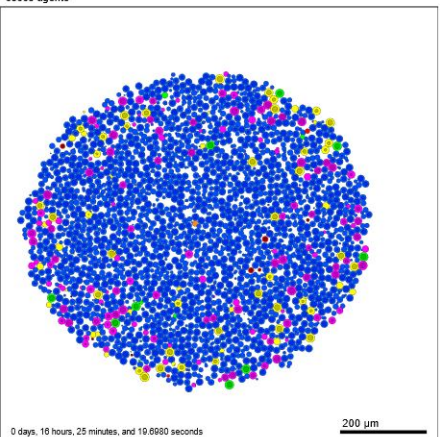
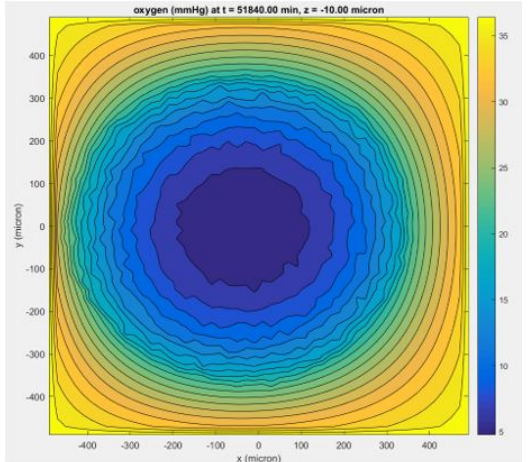
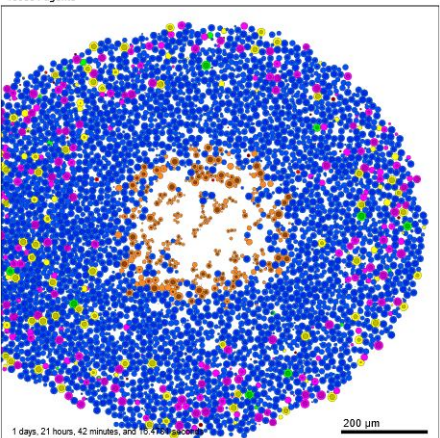


Figure 5.1 3-D Tumor Growth Structure. Yellow cells represent proliferated cells, red cells are apoptotic cells and brown cell are necrotic cells.

5.3 Effect of Initial Oxygen Concentration in the Tumor Microenvironment

Initial oxygen level is 38 mmHg at the beginning of the simulation microenvironment. Initial oxygen is spread all around the microenvironment with the level between 37 mmHg at the borders and 38 mmHg at the center. This oxygen level is appropriate for the cell proliferation without necrosis and cell hypoxia as described in Table 2.1. When tumor structure grows in time in the simulation microenvironment, oxygen level decreases gradually at the place that cell density becomes higher as shown in the Table 5.3. Oxygen level is 5mmHg and lower due cell population at the center of the 3D cartesian mesh. That oxygen level causes the hypoxia in the cell and trigger the necrosis on the hypoxic cells. Necrosis increases in the cells remaining inside of the tumor sphere due to lack of oxygen and a necrotic structure including calcified core and cell loss occurs in the certain places at the center of the tumor spheroid.

Table 5.3
 Oxygen Distribution in the Tumor Microenvironment Over Time.

Oxygen Distribution in the Tumor Microenvironment	Tumor Growth Visual Output
	<p>Current time: 0 days, 0 hours, and 0.00 minutes, z = 0.00 μm 4 agents</p>  <p>0 days, 0 hours, 0 minutes, and 0.0434 seconds</p>
	<p>Current time: 36 days, 2 hours, and 0.00 minutes, z = 0.00 μm 53665 agents</p>  <p>0 days, 16 hours, 25 minutes, and 19.6900 seconds</p>
	<p>Current time: 45 days, 7 hours, and 0.00 minutes, z = 0.00 μm 150584 agents</p>  <p>1 days, 21 hours, 42 minutes, and 16.4760 seconds</p>

5.4 Effect of Initial Oxygen Concentration on the Tumor Growth Rate

Initial oxygen level has been increased up to 50 mmHg from 38 mmHg in the simulation microenvironment in order to see the impact of the initial oxygen level on the tumor growth rate and necrosis structure formation.

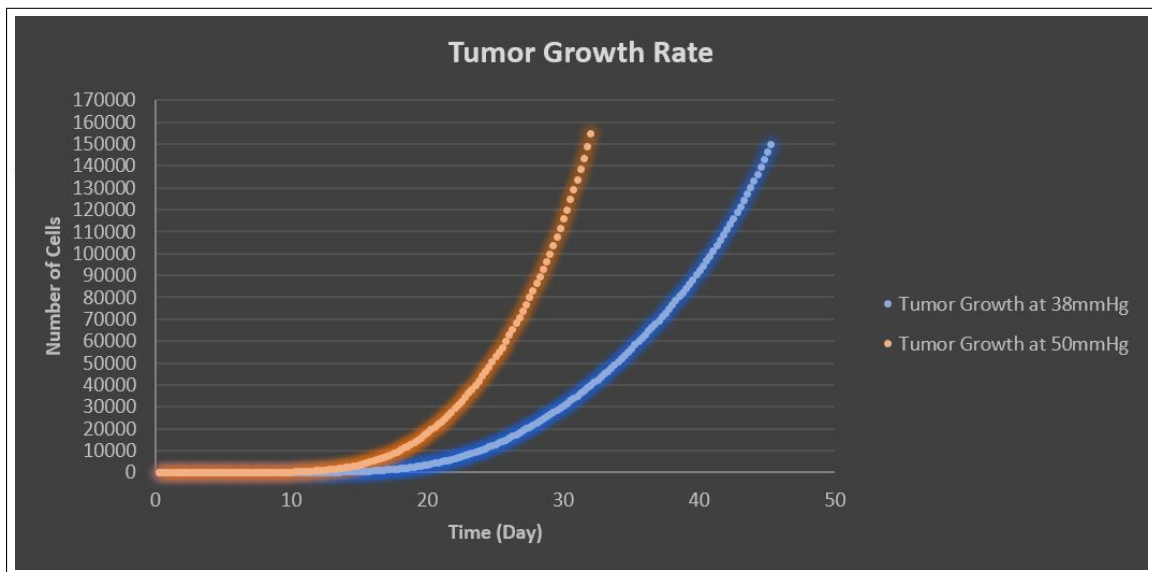
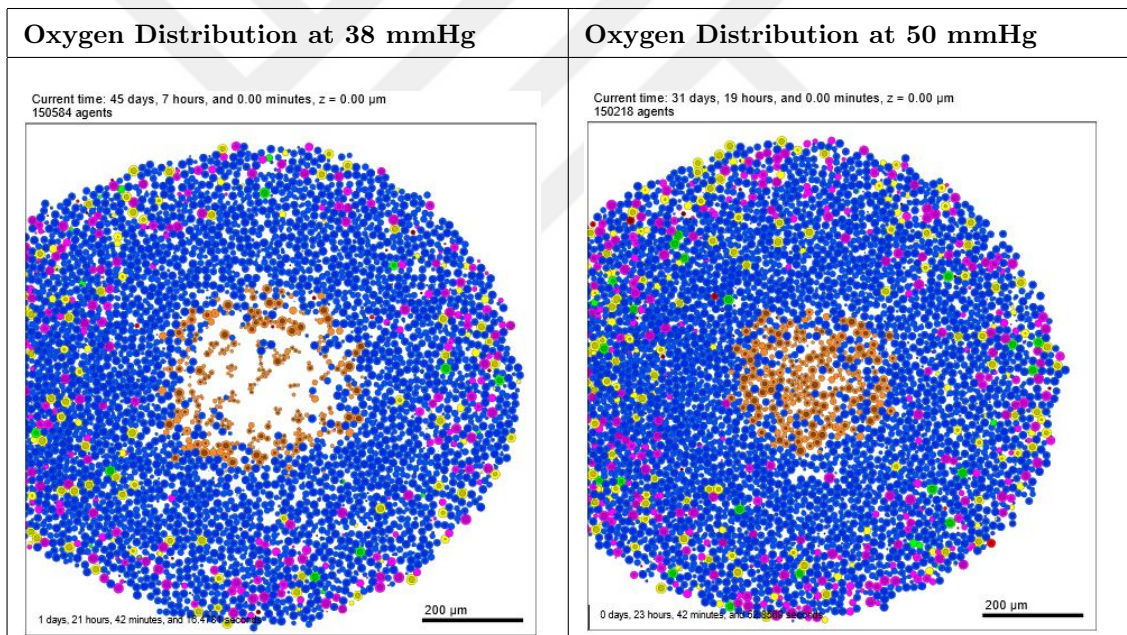


Figure 5.2 Tumor Growth Rate at 38 mmHg and 50 mmHg Initial Oxygen Concentration.

Tumor growth rate increases with the higher oxygen level in the microenvironment as described in Figure 5.2. Tumor spheroid achieve approximately 150.000 cells within 30 days at 50mmHg initial oxygen level and it is 45 days at 38mmHg level as illustrated in Table 5.4. The main reason of this growth rate difference is the penetration of higher amount of oxygen level into the inside of the tumor spheroid. Oxygen drops below 5mmHg level at the inside of the tumor spheroid later than the microenvironment that has 38mmHg initial oxygen level and necrosis process has been formed in the cells later related to oxygen drop.

Table 5.4
Tumor Structure that comprises 150,000 A549 Cells at 38 mmHg and 50 mmHg Initial Oxygen Concentration.



6. DISCUSSION

6.1 Main Findings

We searched eleven open source software for tumor growth modelling as agent-based models as shown in Table 5.1. These agent-based models were classified into two main groups based on their method. Five of the software have lattice-based infrastructure. And, other five of them have off-lattice based basis and one of them have both methods. These methods specify the approaches that are used by the software. Each approach has been defined for each software. Researchers can select the appropriate software based on method and approach used by the software for their study need [11],[13]. Moreover, the inputs that were used in the literature for the software have been searched. Based on the literature, basic cell rules (cell proliferation etc) are used in the all softwares. However, only two of them which are Physicell and Biocellion use the intratumor heterogeneity as the input. Nine of them except Morpheus and Tissue Simulation Toolkit may use the substrate concentration (glucose and oxygen) in the microenvironment. Output has been searched in terms of dimensional, morphology and vascularization. Three dimensional and vascular tumor structure only encoded by Chaste, CompuCell3D, EPISIM and Timothy. Hence, researchers who study the tumor angiogenesis can use these four software.

We developed a 3-D tumor spheroid model using the adeno carcinoma cell specific parameters in the tumor microenvironment. Initial oxygen concentration is accepted as 38 mmHg in the first simulation trial due to oxygen concentration in the peripheral tissues in the human body [1].Based on the initial oxygen concentration (38 mmHg) in the microenvironment, tumor structure achieved approximately $800\mu\text{m}$ diameter with 150.584 cells as shown in Table 5.2. Growing tumor structure also shows necrotic core formation in the tumor spheroid due to oxygen concentration decrease with the increasing tumor diameter in time. The cells went to hypoxia where oxygen concentration is below 8mmHg. Hypoxic cells were subjected to necrosis and necrotic

cells lose their shape integrity and volume. This cause some non-living sections in the necrotic core with the aggregation of cell substances. These non-living sections have been observed after the necrosis in the simulation output as illustrated in last line of Table 5.2 as non-coloring places in the necrotic core.

In order to understand the effect of initial oxygen concentration in the microenvironment, initial oxygen concentration was increased up to 50 mmHg. The cells in the tumor structure proliferated faster than 38 mmHg initial concentration. Since, the higher oxygen amount can penetrate inside the tumor spheroid and the cells became necrotic later as expected. In the 50 mmHg concentration, tumor structure achieved 150.000 cells in 31 days and it was 45 days in 38 mmHg. This rapid growth in 50 mmHg initial oxygen concentration clearly shows the positive effect on the tumor growth. However, higher amount of oxygen delays the HIF-1 α secretion by the tumor cells and adaptation period and survival capability of tumor cells can be lower than the cells in the 38mmHg initial oxygen concentration [38].

6.2 Clinical Applications and Benefits

Hypoxic cells make the cancer treatments more challenging due to their survival capabilities. In recent studies, hypoxia-activated prodrugs have been studied to eradicate the hypoxic cells in order to reduce the tumor survival capabilities [39]. Our simulations can guide the researchers to predict the number of hypoxic cells in the tumor structure to arrange the efficient dose of drugs.

The nitroimidazoles is the one of the substances that target the hypoxic cells. The nitroimidazoles make the hypoxic cells more sensitive the radiation [40]. The dose of the drug can be arranged and predicted using the simulation before radiotherapy in order to increase the rate of success. Since, hypoxic regions in the tumor microenvironment and the day that hypoxia starts in the tumor structure can be found in the simulation outputs. These radiotherapy agents can be used based on the hypoxic regions in the simulation with the optimized time points and the certain amounts that

affect all hypoxic cells [41].

Moreover, tumor progression rate with the certain initial parameters can be calculated in the simulation environment for the patient specific. One of the main initial parameters is the oxygen concentration. And, oxygen concentration varies in the peripheral tissues [5]. Physician may use the simulation to predict the tumor growth rate based on the tumor location to determine the tumor excision time based on the size of tumor structure [3].

6.3 Limitations

Our simulations have been focused on the growth of avascular tumors, whose size is much smaller than that of a clinically detectable tumors (with more than 10^8 cells) due to computational capacity. Greater tumor simulation can be achieved with the super computers. Avascular tumor simulations only give output using the cell-cell and cell-ECM interactions. However, tumor progression is also dependent on the cell vascularization (angiogenesis). Hence, simulations will be improved considering the vascularization effects. Physicell v1.6.1 only simulates the tumor progression based on the initial cell and environmental parameters. Hence, tumor morphology is not identified clearly using Physicell v1.6.1. Morphological features of tumor also will be investigated in the simulation environment with the other open source softwares with different approaches like immersed boundary approaches. Since, center-based model (CBM) that is used by Physicell is not appropriate for the detailed morphological features [42]. Since, cell elongation related morphological features is not directly simulated by Physicell [32]. Simulating morphological features is important due to identified relationship between oxygen concentration and tumor morphology. This morphological effect was studied by Gerlee and Anderson [43]. In their model, they observed that tumor structure has smooth and regular shape features in the tumor microenvironment that has high oxygen concentration and tumor has the shape like fingering in the low oxygen concentration area.

7. CONCLUSIONS

We researched the open source software for the tumor growth simulations considering their input and outputs. The software capabilities and output data have been compared in a tabulated format and the studies which were used the listed software have been explained. Based on the comparison and the literature data, researcher can choose the correct simulation software for their needs in terms of method, approach, input and output.

Moreover, Physicell v1.6.1 has been used to make a 3-D avascular tumor growth simulation that has A549 adeno carcinoma specific cell parameters. Simulations have been completed with 150.543 cells and the approximately $800\mu\text{m}$ tumor and $400\mu\text{m}$ necrotic core diameter in 1 day and 24 hours simulation time that represents 45 days real time. Based on the simulation, the proliferative, quiescent, apoptotic and necrotic cell have been observed. Necrosis has been occurred after 16 hours simulation time and 36 days real time at the center of the tumor spheroid in the simulation environment due to oxygen decrease. Necrotic core in the simulation comprise hypoxic cells. These hypoxic cells have been examined in different microenvironmental conditions to create a correlation between the initial oxygen concentration and hypoxia. Initial oxygen concentration was increased up to 50 mmHg from 38 mmHg. This impact accelerated the cell proliferation and tumor structure achieved 150.000 cells in 31 days real time with smaller necrotic core which is approximately $200\mu\text{m}$ diameter. Since, higher amount of initial oxygen concentration was penetrated into tumor center with the higher concentration. This penetration delays the necrosis and hypoxia in the tumor spheroid and resulted with smaller necrotic structure. Initial oxygen concentration simulation results prove that there is a positive correlation with oxygen concentration and cell proliferation, and also the higher oxygen concentration has negative impact on the tumor necrotic formation. There results show that the simulation results are consistent with the tumor biology in terms of hypoxia in the tumor [5]. These hypoxic regions can be used by the physicians to predict and plan their treatment and surgical

options in future. Since, chemotherapy agents mostly interrupt the cell cycles in the different phases. However, hypoxia prevent the cell proliferation and cause quiescence in the cell. This effect of hypoxia reduces the effectiveness of chemotherapy agents [34]. In order to create an optimized timing for the chemotherapy treatments, number of cells that is subjected to hypoxia and the time that hypoxia occurs can be predicted from the simulation outputs [44] [41].

To sum up;

- Simulations comply with the theory related to hypoxia [1].
- Simulations can replace the cell culture experiments for education purposes for life science students.
- The students can control the following parameters: Cell level: Cell volume (μm^3), Duration of cell proliferation (hour), hypoxia threshold (mmHg), necrosis threshold (mmHg), proliferation threshold (mmHg). Microenvironment: Initial oxygen level (mmHg), glucose level (dimensionless). Simulation level parameters: diffusion_dt (min), mechanics_dt (min), phenotype_dt (min) etc.
- The students can learn the effect of these parameters on tumor growth rate, extent of hypoxia, timing of hypoxia and necrosis formation, oxygen distribution in the tumor microenvironment.
- Excision timing of the tumor can be planned based on the tumor growth rate and measured parameters [3].
- Chemotherapy intervals and dose adjustments can be arranged based on the hypoxic regions [34].
- Radiotherapy planning can be made based on the hypoxic regions [3].
- These techniques may be useful in the clinical practice if more parameters and variables (example: angiogenesis etc.) Less computational need User friendliness
- Simulations may be useful for the personalization of therapy

APPENDIX A. General Code Structure of Tumor Growth Simulation

```

PhysiCell_settings version="devel-version">
  <domain>
    <x_min>-500</x_min>
    <x_max>500</x_max>
    <y_min>-500</y_min>
    <y_max>500</y_max>
    <z_min>-500</z_min>
    <z_max>500</z_max>
    <dx>20</dx>
    <dy>20</dy>
    <dz>20</dz>
    <use_2D>>false</use_2D>
  </domain>

  <overall>
    <max_time units="min">144000</max_time>
    <time_units>min</time_units>
    <space_units>micron</space_units>

    <dt_diffusion units="min">0.01</dt_diffusion>
    <dt_mechanics units="min">0.1</dt_mechanics>
    <dt_phenotype units="min">6</dt_phenotype>
  </overall>

  <parallel>
    <omp_num_threads>8</omp_num_threads>
  </parallel>

  <save>
    <folder>output</folder>

    <full_data>
      <interval units="min">360</interval>
      <enable>>true</enable>
    </full_data>

    <SVG>
      <interval units="min">60</interval>
      <enable>>true</enable>
    </SVG>

    <legacy_data>
      <enable>>false</enable>
    </legacy_data>
  </save>

  <microenvironment_setup>
    <variable name="oxygen" units="mmHg" ID="0">
      <physical_parameter_set>
        <diffusion_coefficient
units="micron^2/min">100000.0</diffusion_coefficient>
        <decay_rate units="1/min">.1</decay_rate>
      </physical_parameter_set>
      <initial_condition units="mmHg">50</initial_condition>
      <Dirichlet_boundary_condition units="mmHg"
enabled="true">38</Dirichlet_boundary_condition>
    </variable>
  </microenvironment_setup>

  <user_parameters>
    <random_seed type="int" units="dimensionless">0</random_seed>
  </user_parameters>

  cell_defaults.functions.cycle_model = flow_cytometry_separated_cycle_model
  cell_defaults.functions.update_phenotype = update_cell_and_death_parameters_O2_based;
</PhysiCell_settings>

```

REFERENCES

1. McKeown, S., “Defining normoxia, physoxia and hypoxia in tumours—implications for treatment response,” *The British Journal of Radiology*, Vol. 87, no. 1035, p. 20130676, 2014.
2. Hockel, M., and P. Vaupel, “Tumor hypoxia: definitions and current clinical, biologic, and molecular aspects,” *Journal of the National Cancer Institute*, Vol. 93, no. 4, pp. 266–276, 2001.
3. Enderling, H., M. A. Chaplain, A. R. Anderson, and J. S. Vaidya, “A mathematical model of breast cancer development, local treatment and recurrence,” *Journal of Theoretical Biology*, Vol. 246, no. 2, pp. 245–259, 2007.
4. Cristini, V., and J. Lowengrub, *Multiscale modeling of cancer: an integrated experimental and mathematical modeling approach*, Cambridge University Press, 2010.
5. Carreau, A., B. E. Hafny-Rahbi, A. Matejuk, C. Grillon, and C. Kieda, “Why is the partial oxygen pressure of human tissues a crucial parameter? small molecules and hypoxia,” *Journal of Cellular and Molecular Medicine*, Vol. 15, no. 6, pp. 1239–1253, 2011.
6. Knudson, A. G., “Cancer genetics,” *American Journal of Medical Genetics*, Vol. 111, no. 1, pp. 96–102, 2002.
7. Deisboeck, T. S., Z. Wang, P. Macklin, and V. Cristini, “Multiscale cancer modeling,” *Annual Review of Biomedical Engineering*, Vol. 13, pp. 127–155, 2011.
8. Network, T. P. S.-O. C., D. B. Agus, J. F. Alexander, W. Arap, S. Ashili, J. E. Aslan, R. H. Austin, V. Backman, K. J. Bethel, R. Bonneau, *et al.*, “A physical sciences network characterization of non-tumorigenic and metastatic cells,” *Scientific Reports*, Vol. 3, p. 1449, 2013.
9. Metzcar, J., Y. Wang, R. Heiland, and P. Macklin, “A review of cell-based computational modeling in cancer biology,” *JCO Clinical Cancer Informatics*, Vol. 2, pp. 1–13, 2019.
10. Norton, K.-A., C. Gong, S. Jamalian, and A. S. Popel, “Multiscale agent-based and hybrid modeling of the tumor immune microenvironment,” *Processes*, Vol. 7, no. 1, p. 37, 2019.
11. Van Liedekerke, P., M. Palm, N. Jagiella, and D. Drasdo, “Simulating tissue mechanics with agent-based models: concepts, perspectives and some novel results,” *Computational Particle Mechanics*, Vol. 2, no. 4, pp. 401–444, 2015.
12. Moreira, J., and A. Deutsch, “Cellular automaton models of tumor development: a critical review,” *Advances in Complex Systems*, Vol. 5, no. 02n03, pp. 247–267, 2002.
13. Van Liedekerke, P., A. Buttenschön, and D. Drasdo, “Off-lattice agent-based models for cell and tumor growth: numerical methods, implementation, and applications,” in *Numerical Methods and Advanced Simulation in Biomechanics and Biological Processes*, pp. 245–267, Elsevier, 2018.
14. Andasari, V., R. T. Roper, M. H. Swat, and M. A. Chaplain, “Integrating intracellular dynamics using compucell3d and bionetsolver: applications to multiscale modelling of cancer cell growth and invasion,” *PloS One*, Vol. 7, no. 3, 2012.

15. Mirams, G. R., C. J. Arthurs, M. O. Bernabeu, R. Bordas, J. Cooper, A. Corrias, Y. Davit, S.-J. Dunn, A. G. Fletcher, D. G. Harvey, *et al.*, “Chaste: an open source c++ library for computational physiology and biology,” *PLoS Computational Biology*, Vol. 9, no. 3, 2013.
16. Mirams, G. R., A. G. Fletcher, P. K. Maini, and H. M. Byrne, “A theoretical investigation of the effect of proliferation and adhesion on monoclonal conversion in the colonic crypt,” *Journal of Theoretical Biology*, Vol. 312, pp. 143–156, 2012.
17. Wilensky, U., and W. Rand, *An introduction to agent-based modeling: modeling natural, social, and engineered complex systems with NetLogo*, Mit Press, 2015.
18. Mansury, Y., and T. S. Deisboeck, “The impact of search precision in an agent-based tumor model,” *Journal of Theoretical Biology*, Vol. 224, no. 3, pp. 325–337, 2003.
19. Shengjun, W., G. Yunbo, S. Liyan, L. Jinming, and D. Qinkai, “Quantitative study of cytotoxic t-lymphocyte immunotherapy for nasopharyngeal carcinoma,” *Theoretical Biology and Medical Modelling*, Vol. 9, no. 1, p. 6, 2012.
20. Swat, M. H., G. L. Thomas, A. Shirinifard, S. G. Clendenon, and J. A. Glazier, “Emergent stratification in solid tumors selects for reduced cohesion of tumor cells: a multi-cell, virtual-tissue model of tumor evolution using compucell3d,” *PloS One*, Vol. 10, no. 6, 2015.
21. La Rosa, L. E. C., D. A. Z. Pareja, F. D. R. Pérez, G. E. Domech, and A. H. Méndez, “Experiences in the use of the compucell3d in the career of biomedical engineering,” in *VI Latin American Congress on Biomedical Engineering CLAIB 2014, Paraná, Argentina 29, 30 & 31 October 2014*, pp. 199–202, Springer, 2015.
22. Giverso, C., M. Scianna, L. Preziosi, N. L. Buono, and A. Funaro, “Individual cell-based model for in-vitro mesothelial invasion of ovarian cancer,” *Mathematical Modelling of Natural Phenomena*, Vol. 5, no. 1, pp. 203–223, 2010.
23. Andasari, V., R. T. Roper, M. H. Swat, and M. A. Chaplain, “Integrating intracellular dynamics using compucell3d and bionetsolver: applications to multiscale modelling of cancer cell growth and invasion,” *PloS One*, Vol. 7, no. 3, 2012.
24. Sütterlin, T., E. Tsingos, J. Bensaci, G. N. Stamatias, and N. Grabe, “A 3d self-organizing multicellular epidermis model of barrier formation and hydration with realistic cell morphology based on epism,” *Scientific Reports*, Vol. 7, p. 43472, 2017.
25. Köhn-Luque, A., W. De Back, J. Starruß, A. Mattiotti, A. Deutsch, J. M. Pérez-Pomares, and M. A. Herrero, “Early embryonic vascular patterning by matrix-mediated paracrine signalling: a mathematical model study,” *PLoS One*, Vol. 6, no. 9, 2011.
26. Merks, R. M., and J. A. Glazier, “A cell-centered approach to developmental biology,” *Physica A: Statistical Mechanics and its Applications*, Vol. 352, no. 1, pp. 113–130, 2005.
27. Daub, J. T., and R. M. Merks, “Cell-based computational modeling of vascular morphogenesis using tissue simulation toolkit,” in *Vascular Morphogenesis*, pp. 67–127, Springer, 2015.
28. Kang, S., S. Kahan, J. McDermott, N. Flann, and I. Shmulevich, “Biocellion: accelerating computer simulation of multicellular biological system models,” *Bioinformatics*, Vol. 30, no. 21, pp. 3101–3108, 2014.

29. Tasseff, R., B. Aguilar, S. Kahan, S. Kang, C. C. Bascom, and R. J. Isfort, “An integrated multiscale, multicellular skin model,” *BioRxiv*, p. 830711, 2019.
30. Li, X., A. Upadhyay, A. Bullock, T. Dicolandrea, J. Xu, R. Binder, M. Robinson, D. Finlay, K. Mills, C. Bascom, *et al.*, “Skin stem cell hypotheses and long term clone survival—explored using agent-based modelling,” *Scientific Reports*, Vol. 3, p. 1904, 2013.
31. Kang, G., C. Márquez, A. Barat, A. T. Byrne, J. H. Prehn, J. Sorribes, and E. César, “Colorectal tumour simulation using agent based modelling and high performance computing,” *Future Generation Computer Systems*, Vol. 67, pp. 397–408, 2017.
32. Ghaffarizadeh, A., R. Heiland, S. H. Friedman, S. M. Mumenthaler, and P. Macklin, “Physicell: an open source physics-based cell simulator for 3-d multicellular systems,” *PLoS Computational Biology*, Vol. 14, no. 2, p. e1005991, 2018.
33. Cytowski, M., and Z. Szymanska, “Large-scale parallel simulations of 3d cell colony dynamics,” *Computing in Science & Engineering*, Vol. 16, no. 5, pp. 86–95, 2014.
34. Powathil, G. G., K. E. Gordon, L. A. Hill, and M. A. Chaplain, “Modelling the effects of cell-cycle heterogeneity on the response of a solid tumour to chemotherapy: biological insights from a hybrid multiscale cellular automaton model,” *Journal of Theoretical Biology*, Vol. 308, pp. 1–19, 2012.
35. von Eichborn, J., A. L. Woelke, F. Castiglione, and R. Preissner, “Vaccimm: simulating peptide vaccination in cancer therapy,” *BMC Bioinformatics*, Vol. 14, no. 1, p. 127, 2013.
36. Ghaffarizadeh, A., S. H. Friedman, and P. Macklin, “Biofvm: an efficient, parallelized diffusive transport solver for 3-d biological simulations,” *Bioinformatics*, Vol. 32, no. 8, pp. 1256–1258, 2016.
37. Jiang, R.-D., H. Shen, and Y.-J. Piao, “The morphometrical analysis on the ultrastructure of a549 cells,” *Rom. J. Morphol. Embryol*, Vol. 51, pp. 663–667, 2010.
38. Ferreira, M. A., E. R. Gamazon, F. Al-Ejeh, K. Aittomäki, I. L. Andrulis, H. Anton-Culver, A. Arason, V. Arndt, K. J. Aronson, B. K. Arun, *et al.*, “Genome-wide association and transcriptome studies identify target genes and risk loci for breast cancer,” *Nature Communications*, Vol. 10, no. 1, pp. 1–18, 2019.
39. Evans, M. A., C. W. Shields IV, V. Krishnan, L. L.-W. Wang, Z. Zhao, A. Ukidve, M. Lewandowski, Y. Gao, and S. Mitragotri, “Macrophage-mediated delivery of hypoxia-activated prodrug nanoparticles,” *Advanced Therapeutics*, p. 1900162.
40. Willers, H., and I. Eke, “Molecular targeted radiosensitizers: Opportunities and challenges,” 2020.
41. Tyson, J. J., and B. Novak, “Regulation of the eukaryotic cell cycle: molecular antagonism, hysteresis, and irreversible transitions,” *Journal of Theoretical Biology*, Vol. 210, no. 2, pp. 249–263, 2001.
42. Osborne, J. M., A. G. Fletcher, J. M. Pitt-Francis, P. K. Maini, and D. J. Gavaghan, “Comparing individual-based approaches to modelling the self-organization of multicellular tissues,” *PLoS Computational Biology*, Vol. 13, no. 2, p. e1005387, 2017.
43. Gerlee, P., and A. R. Anderson, “A hybrid cellular automaton model of clonal evolution in cancer: the emergence of the glycolytic phenotype,” *Journal of Theoretical Biology*, Vol. 250, no. 4, pp. 705–722, 2008.

44. Novák, B., and J. J. Tyson, "A model for restriction point control of the mammalian cell cycle," *Journal of Theoretical Biology*, Vol. 230, no. 4, pp. 563–579, 2004.

